Title

Proliferation of Adult Human Small Intestinal Epithelial Stem Cells by a GSK-3β Inhibitor, CHIR99021 Encapsulated in Poly Lactic-co-Glycolic Acid Nanoparticles

Author

Francis, Rubina Maria Jenova

Publication Date

2014

Peer reviewed|Thesis/dissertation

UNIVERSITY OF CALIFORNIA

Los Angeles

Proliferation of Adult Human Small Intestinal Epithelial Stem Cells by a GSK-3β Inhibitor, CHIR99021 Encapsulated in Poly Lactic-co-Glycolic Acid Nanoparticles

A thesis submitted in partial satisfaction

of the requirements for the degree of Master of Science

in Bioengineering

by

Rubina Maria Jenova Francis

2014

ABSTRACT OF THE THESIS

Proliferation of Adult Human Small Intestinal Epithelial
Stem Cells by a GSK-3β Inhibitor Encapsulated in
Poly Lactic-co-Glycolic Acid Nanoparticles

by

Rubina Maria Jenova Francis

Master of Science in Bioengineering
University of California, Los Angeles, 2014
Professor James C.Y. Dunn, Chair

Successful identification of 'Lgr5' as a bona fide stem cell marker of small intestinal crypt base columnar (CBC) adult epithelial stem cells is a major breakthrough in the realm of intestinal stem cell biology and regenerative medicine. Although various culture conditions exist to support the growth of intestinal epithelial cells in vitro, no exogenous conditioned media or growth factor is sufficient enough to provide the essential 'niche' signal to sustain growth and proliferation of Lgr5+ stem cells in cultures. More recently, a small molecule inhibitor which is a glycogen synthase kinase 3β (GSK-3β) inhibitor, CHIR99021 was identified as an exogenous factor that contributes toward long-term culture and expansion of mouse small intestinal

epithelial stem cells. This small molecule, by specifically inhibiting the activity of GSK-3β, activates the Wnt/β-catenin (canonical Wnt) pathway which is quintessential for maintaining self-renewal and proliferation of CBC stem cells, simultaneously regulating Notch, BMP, and other cell survival pathways. In an attempt to translate this effect in vivo, this report offers an efficient way to encapsulate this small molecule using a nanoparticulate drug delivery vehicular system (PLGA nanoparticles) aimed for a tissue localized delivery. This work focuses on studying the stemness-retaining effect induced by this inhibitor on adult human small intestinal epithelial cells in vitro. To elucidate the efficacy of PLGA encapsulated CHIR99021, various cell culture experiments were conducted on: (i) lentiviral TCF/LEF reporter transduced spheroids to justify the mechanism that CHIR99021triggers canonical Wnt pathway in adult small intestinal epithelial cells, (ii) non-transduced spheroids to determine the morphological and structural changes (conversion of spheroids to enteroids) induced as a result by activation of Wnt/ β-catenin signaling, (iii) small intestinal crypts to evaluate the proliferation of Lgr5+ stem cells and also their survival in the absence of an apoptotic inhibitor but in the presence of CHIR99021. Overall, this work demonstrates that the small molecule inhibitor encapsulated in PLGA nanoparticles is pharmacologically active and its efficacy is demonstrated by various in vitro experiments on adult human small intestinal epithelial cells.

The thesis of Rubina Maria Jenova Francis is approved.

Benjamin M. Wu

Min Lee

James C.Y. Dunn, Committee Chair

University of California, Los Angeles

2014

TABLE OF CONTENTS

LIST OF FIGURES

LIST OF TABLES

ACKNOWLEDGEMENTS

I would like to remember and thank my God Almighty and Heavenly Mother for guiding me throughout this journey at UCLA. I am grateful to my husband Sujay Irudayaraj and my parents Francis Savier and Vincent Jeyaseeli for their love, encouragement and support.

I would like to express my gratitude to my advisor Dr. James Dunn, for his invaluable support and guidance throughout my thesis project. I would also like to thank Dr. Benjamin Wu and Dr. Min Lee for their counsel and advice in my work. I would also like to thank my lab members for their help and suggestions during my research.

1.1 INTRODUCTION

Engineering small intestinal tissue promises a more viable cure for major intestinal failure and abnormalities. There are some compelling reasons for taking curative efforts to develop small intestinal tissues in a laboratory setup so as to obtain therapeutic remedies to anatomic/functional loss of gastrointestinal tissue, to ameliorate complications resulting from multiple postoperative infections, to cut costs associated with medical and surgical treatments and to improve the overall well-being of the affected individual. Massive loss of intestinal tissue compromises various vital functions including digestion and absorption, thus affecting the overall health of the affected individual. There are several gastrointestinal abnormalities that cause serious complications including dysfunction of an entire segment of the intestine which could potentially result in surgical resection of that portion of the bowel. Such major intestinal tissue loss results in a condition called Short bowel syndrome (SBS) [1, 2]. Typically, more than 70% loss of intestine will result in SBS. Some conditional disorders associated with SBS include Crohn’s disease, mesenteric vascular disease, trauma and desmoid tumor in adults and Hirschsprung's disease, necrotizing enterocolitis, gastroschisis, congenital short bowel, artresias and volvulus in the pediatric population.

SBS is a highly morbid condition characterized by acute failure to maintaining normal gastrointestinal function resulting in malnutrition followed by death, if not supported by parenteral nutrition and/or surgical intervention. Mostly, patients affected by SBS thrive on total parenteral nutrition or enteral nutrition, and surgical interventions or intestinal transplantation. Despite many advanced medical facilities, many patients still suffer therapeutic consequences with no significant improvement in overall life expectancy, since every available treatment option has its own risks and benefits. For example, long-term parenteral nutrition has been

associated with catheter-related sepsis and thrombosis, and notably hepatic and biliary complications [3, 4, 5]. Particularly among pediatric population, average life expectancy compared with the enterally fed children is still considerably lower. Also, there is also a high risk of total intestinal failure associated with parenteral nutrition [6]. But surgical procedures aided to overcome challenges due to parenteral nutrition to some extent. In late 60s, surgical approaches like creating reversed intestinal segments, recirculating small bowel loops, etc., [7, 8] were in use to enhance nutrient absorption but are rarely followed today. Current operative approaches to improve the outcome of patients with SBS involve procedures such as intestinal lengthening and tapering, strictureplasty, creating artificial enteric valves and others. Of the above, longitudinal bowel lengthening (old Bianchi and recent serial transverse enteroplasty) seem to have good prognosis with minimal surgical complications and overcome potentially life-threatening situations involved with parenteral nutrition [9, 10]. Another seemingly curative option for intestinal failure is intestinal transplantation. Though seemed promising at first, post-transplant complications including graft rejection, sepsis, along with life-long immunosuppression have limited this option to be clinically non-viable and necessitate more research to find promising therapeutic solutions for intestinal failure [11].

Efforts were taken to steer research attempts into determining more plausible therapeutic remedies. Certain research group implanted ex vivo developed tissue-engineered small intestine (TESI) in animal models. Rat intestinal epithelial organoid units embedded in PGA scaffolds were implanted into the omentum of syngeneic rats. The results demonstrated survival and proliferation of these epithelial units forming complex cystic structures expressing mature cell types of the epithelium resembling rudimentary intestine [12]. But this approach also has some clinical constraints if it has to be translated to humans: including syngeneic donor availabilities,

large volume of tissue to harvest sufficient organoid units, long-term immune suppression if non-syngeneic tissue is transplanted, and so on. Hence, alternative solutions to the above-discussed problems to treat short gut syndrome still need to be researched upon.

Recently, more concentrated efforts are directed toward regenerative medicine, as stem cells seem to have enormous potential to treat various diseases and injury, for example in bone marrow transplantation. Though more elusive to be tracked and distinguished from other progenitor cells due to lack of molecular markers, recent advancements have provided tools such as, cell position mapping, lineage tracing strategies, clonogenic assays, 'knock-in and knock-out' mouse genetic assays, for identification and isolation of intestinal epithelial stem cells. The inherent self-renewal capability of these stem cells is what helps maintain the epithelium its structure and function. Recent demonstrations of assembling stem cell-driven tissue in culture seem to provide an optimistic relief to SBS. Advancements in the biology and engineering field has offered tools like natural/synthetic polymers and exogenous growth factors to manipulate, grow and regenerate stem cells in a 3D environment into a tissue reminiscent of the native tissue. Successfully transplantation of the ex-vivo developed organoids in humans would be the next highly sought-after goal in the search for a permanent solution to this problem.

Mammalian small intestinal epithelium is the most rapid self-renewing rapid turnover time of about 4 to 5 days [13]. Intestinal epithelium comprises of two distinct compartments - crypts and villi. Crypts are characterized by pit-like recessions homing stem cells at the bottom followed by transit-amplifying (TA) progenitors, the immediate daughter cells emerging from stem cells. Villi are small, finger-like projections composed of differentiated epithelial cells generated from TA progenitors. There are 4 major terminally differentiated epithelial cell types found in the epithelium: the absorptive enterocytes, mucus-secreting goblet cells, hormone-

secreting enteroendocrine cells and anti-microbial peptide-secreting Paneth cells. Paneth cells are the only differentiated cells found adjacent to the stem cells at the bottom of the crypts, while the other three cell types are found lining the villi. The TA progenitors, as they divide and get terminally differentiated into any of the epithelial cell types, move up along the villi and are eventually shed into the lumen and replaced with fresh epithelial cells (Fig. 1) [14]. Thus, these four types of differentiated cells along with crypt-residing stem cells make the small intestinal epithelium. So far, two types of intestinal stem cells (ISCs) have been defined: small, rapid cycling crypt-base columnar cells (CBC) and quiescent '+4' stem cells. CBC cells, interspersed between the Paneth cells, are one group of ISCs found to specifically express Wnt target gene Lgr5 (leucine-rich repeat-containing, G-protein-coupled receptor) both in mice and human [15-17]. *Olfactomedi-4* (Olfm-4) has also been found as another specific marker for lgr5-type (rapid-cycling) stem cells [23]. While the quiescent stem cells are identified with markers like *Bmi1*, a *Polycomb group*, *Tert*, *Hopx* and *Lrig1* [18-21]. But, in a recent study Lgr5+ stem cells also have been reported to express all '+4' stem cell markers [15]. Lgr5+ ISCs attain proliferative state much faster than the Bmi1-labeled ones terming the former as 'proliferative' and the latter as 'quiescent'. Also, under normal conditions, Lgr5+ stem cells are found to be responsible for renewing the epithelium. Whereas 'quiescent' stem cells and other progenitor cell population (DLL1+ secretory progenitor and LGR5+ label retaining Paneth cell progenitor) take over by regenerating Lgr5+ stem cells, when Lgr5+ CBC stem cells are lost due to inflammation or injury. These are the 'reserve' source of stem cells. Thus, these two groups of stem cells synergistically maintain homeostasis of the entire small intestinal epithelium [18, 24, 25, 52].

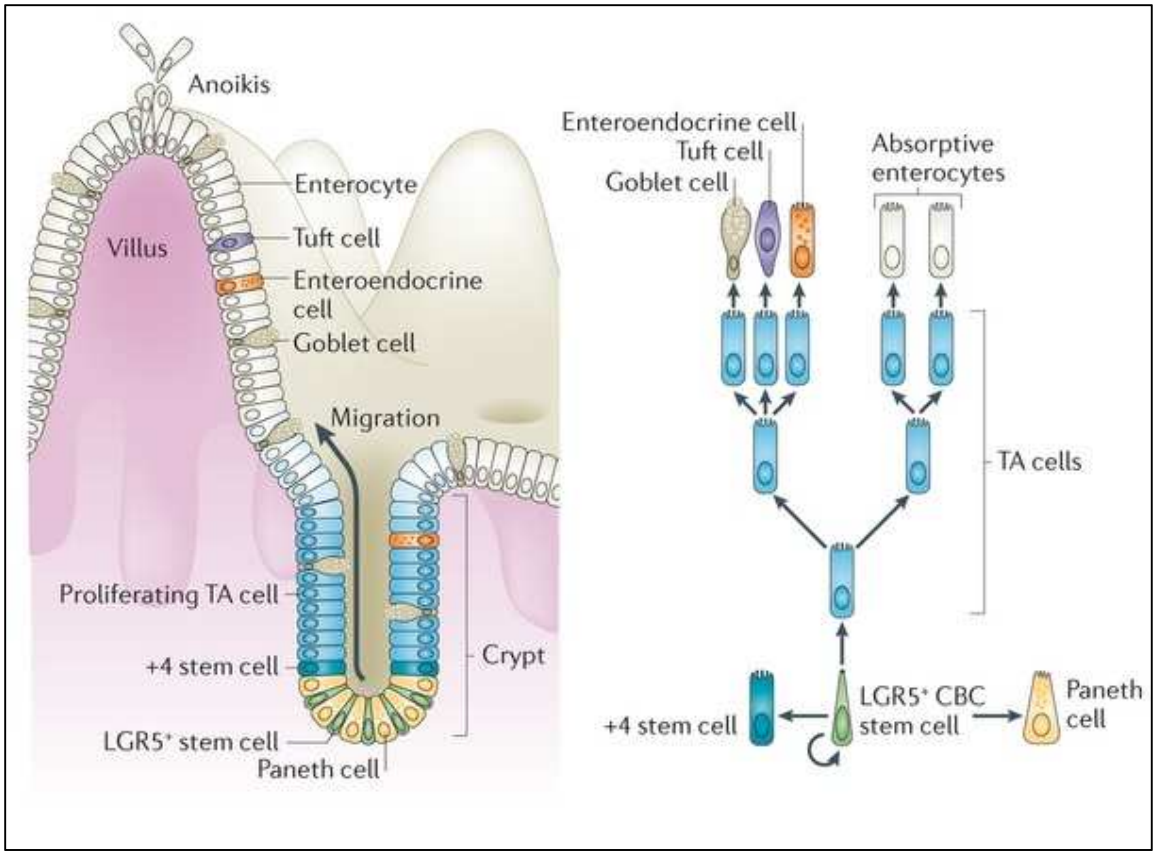

Figure 1. Epithelial self-renewal in the intestinal epithelium. In the small intestine, LGR5+ (Leu-rich repeat-containing G protein-coupled receptor 5-expressing) crypt base columnar (CBC) stem cells are intercalated with Paneth cells at the crypt base. These stem cells continuously generate rapidly proliferating transit-amplifying (TA) cells, which occupy the remainder of the crypt. TA cells differentiate into the various functional cells on the villi (enterocytes, tuft cells, goblet cells and enteroendocrine cells) to replace the epithelial cells being lost via anoikis at the villus tip. The +4 'reserve' stem cells (which occupy the fourth position from the crypt base) can restore the LGR5+ CBC stem cell compartment following injury. This differentiating hierarchy is shown in the tree on the right panel. Epithelial turnover occurs every 3–5 days. New Paneth cells are supplied from the TA cells every 3–6 weeks (adapted from Nick Barker, [52]).

Many complex signaling pathways such as Wnt, Notch, Hedgehog (Hh), and BMP coordinate and regulate the fate of the intestinal epithelial cells [32-34]. Of these, Wnt signaling together with Notch is important in controlling stem cells and BMP and Hh drive differentiation of these stem cells [32].

Studies in the recent years demonstrated cell culture conditions for developing small intestinal organoids derived from crypts and stem cells isolate from crypts. Sato et al reported

that single sorted Lgr5+ stem cells developed into small epithelial organoids which were identified to consist of all four cell types of the epithelium, simply representing miniature gut [26, 27]. Also, another parallel study showed that organoids derived from Lgr5+ colon stem cells expanded indefinitely in culture for longer period. Subsequently, when the organoids were transplanted in an inflamed mouse colon, they formed a layer of epithelium resembling native intestine with crypts and all differentiated cell types [28]. Several other studies also have demonstrated similar success in transplanting fetal intestinal progenitors in regenerating colon epithelium [29], engraftment of autologous intestinal organoids developing neomucosa in dogs [30], and so on. Besides therapeutic reasons, lab-made intestinal organoids are also used as tissue surrogates for toxicological and pharmacological studies [31].

Even though culture conditions exist for culturing intestinal crypts, culture media alone is not sufficient to sustain self-renewal of the stem cells in vitro. Some exogenous factors are necessary to retain stem cells in culture. Two such factors, small molecule inhibitors (CHIR99021 and valproic acid) were identified to maintain self-renewal and increase colony forming efficiency of mouse intestinal epithelial stem cells in culture. Notably, they were cultured independent of essential stem cell 'niche' in the presence of these small molecules [53]. In another independent study, CHIR99021 has been reported to dramatically improve the colony forming efficiency of isolated human intestinal stem cells [36]. In this report, this small molecule's ability in supporting the survival and proliferation of human intestinal epithelial stem cells has been studied.

CHIR99021 is a specific pharmacological inhibitor of glycogen synthase kinase 3β (GSK-3β). GSK-3 is a multifunctional serine/threonine protein kinase involved in regulating various intracellular signal transduction pathways, particularly Wnt/β-catenin signaling pathway.

The protein kinase acts by phosphorylating its substrate molecules, inhibiting it from its targeted activity. GSK-3 is involved in various biological processes such as proliferation, cell fate determination, survival and gene expression by regulating Wnt signaling pathway [37]. To date, 3 major Wnt pathways have been described: canonical (Wnt/β-Catenin) and non-canonical (Wnt/planar cell-polarity and Wnt/calcium) pathway. Of these, GSK-3 is involved in negatively regulating canonical Wnt pathway. In the absence of Wnt signaling, β-Catenin is bound to a group of proteins, GSK-3β, casein kinase 1 (CK-1), tumor suppressor protein Adenomatous Polyposis Coli (APC), and scaffolding protein Axin together called the 'destruction complex'. Under normal conditions, this complex prevents β-Catenin from translocating to the nucleus to activate downstream transcription of Wnt target genes, subjecting it to ubiquitination and proteasomal degradation. This helps maintain low levels of β-Catenin in the cytoplasm. But, upon binding of an extracellular Wnt ligand to the transmembrane receptor Frizzled and its co-receptor LRP-5/6 (Low-density lipoprotein receptor-related protein), the Wnt signaling cascade is activated. Once the signal is initiated, downstream effectors activates a cytosolic protein called Dishevelled (Dsh) to bind to Frizzled receptor that forces dissociation of the destruction complex. No longer can GSK-3β along with other proteins can inhibit β-Catenin from being ubiquitinated and tagged for destruction. The series of cascaded reaction increases the levels of unbound β-Catenin in the cytoplasm which then causes it to translocate to the nucleus. In the nucleus, together with other proteins it replaces Groucho and binds to the TCF/LEF (T cell factor/Lymphoid Enhancer Factor) transcription factors - transcription repressors of Wnt target gene – and finally activates them [38, 39]. The mechanism of action is illustrated in Fig. 2. But, regardless of any Wnt ligand-binding activity to turn the Wnt on, CHIR99021 is capable of stimulating Wnt/ β-Catenin signaling. It acts by inhibiting GSK-3β from phosphorylating β-

Catenin to be liberated from being tagged for destruction. This then calls for various downstream actions to turn the Wnt signaling on. Thus, this small molecule indirectly facilitates stimulation of canonical signaling, which regulates stem cell self-renewal, proliferation and survival. Besides its capability in reprogramming the fate of stem cells, which could possibly be directed for use in regenerative medicine, inhibiting the activity of GSK-3β has desired outcomes in various clinical conditions.

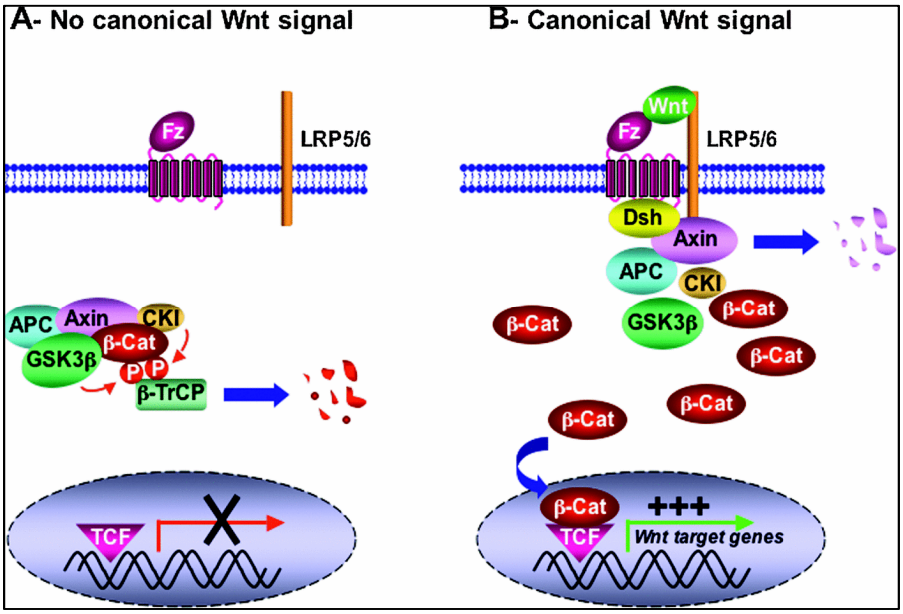

Figure 2. Canonical and Non-Canonical Wnt Signaling Mechanism

(A) In the absence of Wnt ligand, β-catenin is sequestered in a multiprotein degradation complex containing the scaffold protein Axin, the tumour suppressor gene product APC, as well as the kinases CKI and GSK3β, among others. Upon sequential phosphorylation, β-catenin is ubiquitinated by the β-TrCP–E3-ligase complex and subsequently degraded by the proteasome machinery. There is no transcription of *Wnt* target genes. (B) Wnt ligand associates with Fz and LRP5/6 co-receptors. This in turn can lead to translocation of Axin (and perhaps the whole multiprotein complex) to the plasma membrane through direct interaction with LRP5/6 and Dsh/Fz. Translocation results in Axin degradation and/or dissociation of the multiprotein complex. GSK3β also might be displaced from this complex through Dsh action. β-catenin is then released from the multiprotein complex, accumulates in the cytoplasm in a non-phosphorylated form, and subsequently translocates into the nucleus where by association with TCF/LEF factors it promotes transcription of Wnt target genes (adapted from Xi He, 2003 [38], Pinto et al., 2005 [22]).

As dysregulation in phosphorylation of GSK-3β results in aberrant Wnt signaling, it is associated with variety of diseases including type II diabetes, Alzheimer's disease, neurodegeneration, breast, prostate, colorectal cancer and others [40, 41]. In such cases, inhibiting the activity of GSK-3β has resulted improvement in disease conditions.

In order to achieve this small molecule-induced benefit in vivo, this study demonstrates methods to effectively encapsulate it using an appropriate drug delivering matrix to determine its pharmacological effect on small intestinal epithelial cells. Drug delivering matrices are used for controlled/sustained delivery of drugs over a certain period of time. Different polymeric drug delivering systems ranging from hydrogels to nanocarriers like nanoparticles, liposomes, micelles, dendrimers, etc. have been explored so far as potential drug delivery systems. Polymeric drug carriers have a myriad of applications in the field of medicine and pharmaceutical sciences. They are used as a protective carrier for delivering drugs, genes, peptide molecules, vaccines, etc. The primary goal for encapsulating pharmaceutically active agents is to provide protection from the host defense mechanism in order to reach the diseased cell/tissue for prolonged, localized delivery and also reduce possible drug-induced adverse effects to its surroundings. Ideally, a drug delivery system should be biocompatible, biodegradable and accomplish therapeutically-desired outcomes. Nanoscience technology is striving to bring such significant advances amidst various challenges. Among different types of drug carriers, nanoparticles have been in use for decades in the field of drug delivery for various applications from diagnosis to treatment of diseases.

In this study, the small molecule drug is encapsulated using nanoparticles made up of poly lactic-co-glycolic acid (PLGA). PLGA is a widely used copolymer in the manufacturing of various medical equipments such as sutures, grafts and implants, prosthetic devices, surgical

sealants and so on. It is synthesized by ring-opening polymerization of two different monomers, lactic acid and glycolic acid. It degrades by hydrolysis of its ester linkages when exposed to aqueous environments into its monomer units, lactic and glycolic acid which are biodegradable, since they are by-products of various metabolic activities in the body. PLGA has many distinct advantages on its own: (i) biodegradable and biocompatible, (ii) effectively encapsulate hydrophobic and hydrophilic small/macro molecules with controlled/sustained drug release properties, (iii) has surface-modifiable features for stealth purposes and (iv) possibility to attach antibodies for targeting to specific cell/tissue/organs and (v) approved by FDA and European Medicine Agency [42]. Due to its many advantages including flexibility in modifying/designing features for targeting and site-specific delivery, PLGA nanoparticles have been extensively used in cancer therapeutics. It has also been used as ‘dual’ drug carriers carrying MRI contrast agents and anticancer drug for cancer therapy [43, 44]. Thus, PLGA nanoparticulate system represents one of the most advantageous platforms for use in the field of drug delivery.

1.2 OBJECTIVE

The primary goal of this study is to determine the efficacy of PLGA nanoparticles' encapsulated GSK3β inhibitor (CHIR99021) on small intestinal epithelial stem cells for retaining stemness and inducing proliferation of these cells.

Specific Aim 1:

Design and formulate PLGA nanoparticles encapsulating CHIR99021 and characterize physicochemical properties of the nanoparticles and finally, evaluate drug release kinetics.

a. Synthesis of CHIR99021 encapsulated PLGA nanoparticles with good drug loading capacity and encapsulation efficiency.

b. Characterize nanoparticles' size, zeta potential, and surface morphology using SEM.

c. Study drug release characteristics using UV-Vis spectroscopy.

(i) Hypothesis: Given the wide range of drug delivery carriers, nanoparticles manufactured using biodegradable polymers like PLGA, play a central role in the realm of drug delivery therapeutics. Its ability to effectively encapsulate variety of drugs and more pliable formulation features to obtain controlled release of the pharmacological agent suggests that PLGA nanoparticles would be a more viable option for encapsulating CHIR99021, a hydrophobic small molecule. Also, this protocol would be suitable for encapsulation of drugs with similar physical characteristics which alongside CHIR99021 might synergistically help in the small intestinal organogenesis.

Specific Aim 2:

Test the pharmacological efficacy of PLGA nanoparticles-encapsulated CHIR99021 on adult human small intestinal spheroids and small intestinal crypts for morphological and molecular level changes induced by the activation of Wnt/β-catenin signaling, a profound downstream effect of CHIR99021.

a. Establishing small intestinal spheroids in culture by passaging and transfecting them using lenti TCF/LEF reporter and isolating intestinal crypts from tissue.

b. Determining and analyzing dose-dependent effects of CHIR99021 on crypts and spheroids by using various amounts of nanoparticles.

(ii) Hypothesis: The biological activity CHIR99021-embedded PLGA nanoparticles will remain intact to induce its inherent inhibitory effects. Being a hydrophobic and photosensitive small molecule, maintaining CHIR99021's potency is crucial to activating Wnt signaling mechanism to initiate self-renewal and proliferative activity of small intestinal stem cells. Since the formulation methods involve various robust treatments involving dissolution in organic solvent, ultrasonication and overnight solvent evaporation, it is important that the pharmacological activity is maintained for achieving desired signal transduction activation in vitro/ in vivo.

Specific Aim 3:

Conduct real-time quantitative polymerase chain reaction (qRT-PCR) analysis to determine the fold-increase in maintaining stemness and proliferation of small intestinal stem cells induced by PLGA-encapsulated CHIR99021.

(iii) Hypothesis: CHIR99021 targets and simultaneously modulates Wnt, Notch and bone morphogenetic protein pathways to sustain proliferation of intestinal stem cells. Coordinated regulation between these pathways is quintessential for maintaining intestinal homeostasis. Over activation of just one signaling pathway to maintain stemness by preventing adequate differentiation of stem cells into different epithelial cell lineages will not support proper 'wholesome' tissue regeneration. Thus, it is essential to support the growth and development of stem cells, simultaneously controlling differentiation.

2. MATERIALS AND METHODS

2.1 Materials

GSK-3β inhibitor, CHIR99021 (CHIR) was purchased from Stemgent (Cambridge, MA) and dimethylsulfoxide (DMSO) was purchased from American Type Culture Collection (ATCC) (Manassas, VA). Poly(DL-lactide-co-glycolide) (PLGA, lactide:glycolide ratio 85:15, MW: 75,000-100,000 , inherent viscosity (0.55-0.75dL/g) was purchased from Durect Lactel Corporation (Birmingham, AL). Dichloromethane (DCM) (ACS grade), Polyvinyl alcohol (PVA) (Mw: 89,000-98,000) and Sodium dodecyl sulfate (288.4 g/mol) were from Sigma Aldrich (USA).

2.1.1 Preparation of CHIR-loaded PLGA Nanoparticles

PLGA nanoparticles were prepared by single emulsion (oil-in-water) solvent evaporation technique. 200mg of PLGA is dissolved in 6mL (7.98g) of dichloromethane (2.5% w/w) as a stock solution. To 250uL of the above PLGA/DCM solution, 250uL of DCM and 36uL of CHIR dissolved in DMSO (10mM) is added and stirred for about 5 minutes. The aqueous phase is prepared by adding 1% (w/v) PVA solution as emulsifier containing about 0.1% (w/v) SDS. The solution of organic phase along with the drug is then added to the aqueous emulsifier/stabilizer solution dropwise while it is being ultrasonicated at 20% amplitude, 500W. The ultrasonication time is 50 seconds and the process is performed on an ice bath to dissipate heat generated from sonication. The formed oil-in-water emulsion is then gently stirred at room temperature (22°C) at 400rpm by a magnetic stirrer (Corning®, CA) overnight to evaporate the organic solvent and for the PLGA nanoparticles to get hardened. The precipitated PLGA nanoparticles are isolated by centrifugation (Eppendorf, Germany) at 14000rpm for 5 minutes at 4 °C and washed thrice with ultradistilled water to remove excess surfactant and unincorporated drug. The collected

nanoparticles are sterilized by exposure to UV light for about 10 minutes and used for in vitro cell culture experiments [45]. Scheme of preparation is illustrated in Fig. 3. Blank PLGA nanoparticles were fabricated using the same procedure with the exception of using 36uL of DMSO instead of drug solution. Blank nanoparticles were used as control group to subtract the absorbance values of the degradation byproducts of PLGA for the release profile and also in cell culture studies.

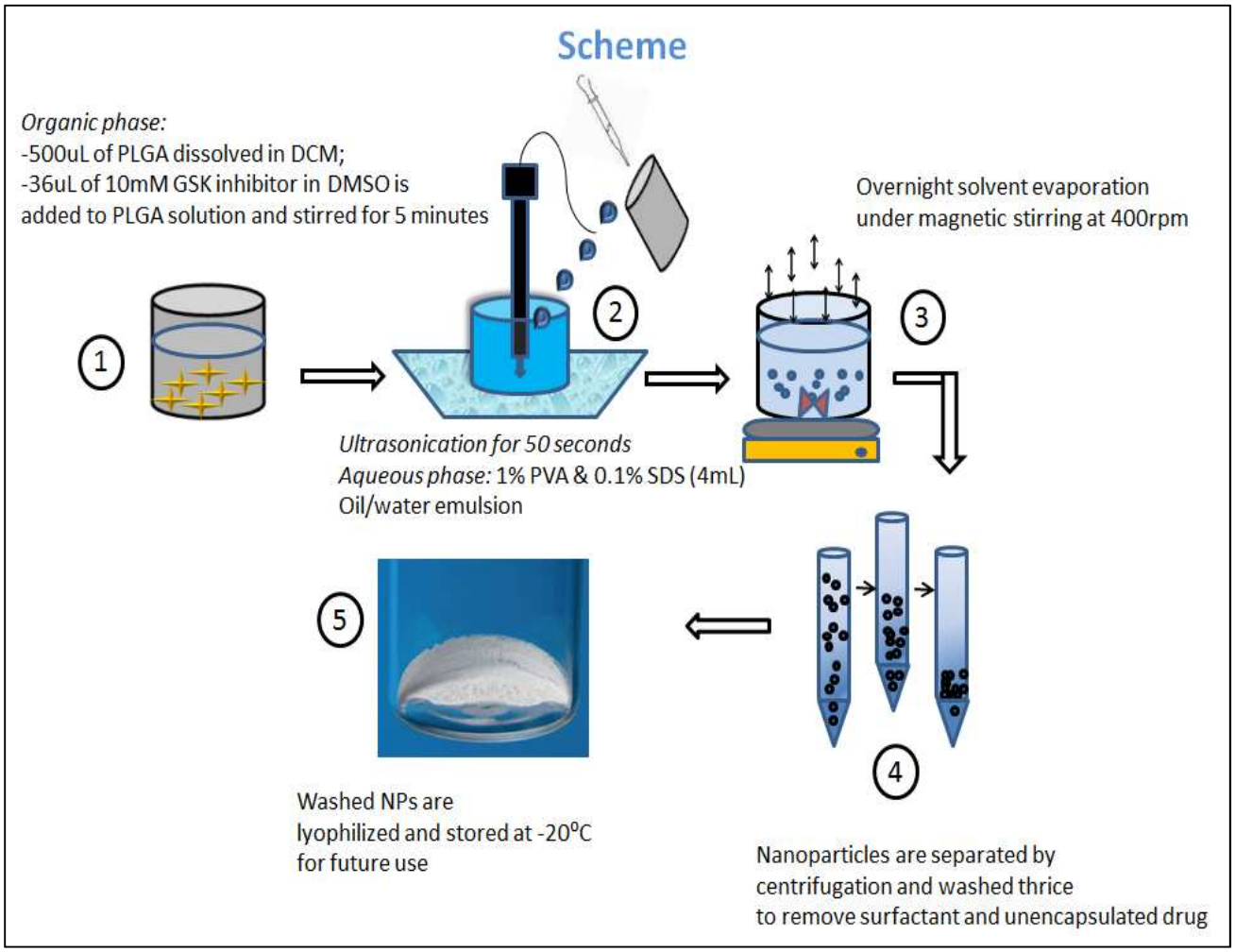

Figure 3. Scheme of PLGA nanoparticles preparation.

2.1.2 Determination of CHIR encapsulation efficiency and nanoparticle yield

CHIR content in the nanoparticles were assayed in triplicates by UV Spectrophotometer (Beckman Coulter, CA). Drug loaded nanoparticles were lyophilized and dissolved in 1mL of DMSO. The mixture is vortexed to ensure complete solubility of the nanoparticles in the solvent. Blank PLGA nanoparticles were also dissolved similarly as a control to subtract the background produced by PLGA from CHIR-loaded particles. Drug content is then quantified by UV detection at 282nm using a standard calibration curve. The encapsulation efficiency and yield is calculated using the formula:

Encapsulation efficiency (EE) % = (Amount of CHIR loaded (nmol)/ Amount of CHIR used originally (nmol)) X 100

Nanoparticle yield = (Experimental dry weight of the nanoparticle precipitate (mg)/ theoretical weight of PLGA (mg)) X 100

2.2 Material characterization

2.2.1 Particles size distribution and Zeta potential

Nanoparticle size distribution - mean diameter and polydispersity index - was analyzed by a dynamic light scattering (DLS) instrument, Zetasizer (Malvern). The analysis was performed at a temperature of 25°C at a scattering angle of 90° using samples appropriately diluted with nanopure water and placed in the measurement cell (clear disposable zeta cell for size and charge measurements).

Nanoparticles were also characterized with respect to electrophoretic mobility and zeta (ζ) potential using the same instrument. The electric field applied was 10 V. Samples were prepared similar to the size determination procedure and evaluated for the surface charge. For each

sample, the average diameter of three determinations was calculated. Values are reported as the mean ± standard deviation for three different batches of CHIR-loaded and blank nanoparticles.

2.2.2 Scanning Electron Microscopy

CHIR-PLGA and blank nanoparticles obtained after purification were lyophilized. Lyophilized nanoparticles were smeared on carbon-coated SEM stubs and imaged with a field emission SEM (NovaNanoSEM230_D9064, FEI, USA) at higher magnifications.

2.3 In vitro release study

The in vitro release kinetics of the nanoparticles was determined in a buffered solution. Known amount of nanoparticles was suspended 0.01M phosphate buffered saline (PBS) and incubated at 37°C throughout. Supernatants were collected after centrifugation at 14,000rpm for 5 minutes at predetermined time intervals for about 2 weeks and replaced with the same volume of fresh PBS. The supernatant was then analyzed using UV-Visible Spectroscopy for amount of CHIR released. Standard curve was plotted using the absorbance values of the standard solutions of different concentrations of CHIR. The amount of drug released was determined using the standard curve.

2.4 In vitro cell culture assay

Two types of cell culture experiments were used to determine the efficacy of CHIR encapsulated nanoparticles:

(i) Human small intestinal spheroids

- Lenti TCF/LEF reporter transduced spheroids
- Non-transduced spheroids

(ii) Human small intestinal crypts

2.4.1 TCF/LEF transduced spheroids and non-transduced spheroids

2.4.1.1 Materials and method

Small intestinal spheroids developed from isolated crypts were embedded in growth factor reduced Matrigel (BD Biosciences, San Jose, CA) and cultured in a 48-well tissue culture plate with 50% of conditioned media from myofibroblasts (Human Batch 8n, HB8n cell line) and other 50% constituting growth factor media. The media comprises of Advanced DMEM/F12 (ADMEM) (Invitrogen, Carlsbad, CA) supplemented with GlutaMax supplement (Invitrogen), HEPES buffer (10mmol/L, Invitrogen), penicillin (100U/mL)/streptomycin (100ug/mL) (Invitrogen), 1x N2 supplement (Invitrogen), 1x B-27 supplement minus Vitamin A (Invitrogen) and N-acetylcysteine (1mmol/L, Sigma St. Louis, MO). Growth factors include epidermal growth factor (EGF, 50ng/mL) (PeproTech, Rock Hill, NJ), murine noggin (200ng/mL), human R-spondin-1 (R&D Systems, Minneapolis, MN, 1mg/mL), fibroblast growth factor 10 (FGF-10, 100ng/mL, R&D Systems) and Rho-kinase inhibitor Y-27632 (10umol/L, Stemgent). Spheroids were transduced with lenti TCF/LEF reporter according to the method as described by Koo et al [46]. Transduced spheroids were cultured for few days until ready to be passaged. They were then mechanically dissociated, replated with Matrigel and grown for about 4 days before adding the differentiation media containing all of the above culture media supplements and growth factors EGF, Noggin, R-spondin1, FGF-10, Y-27632 (collectively, ENRFY) but without myofibroblasts' conditioned media. Different conditions were employed: negative control group with spheroids cultured with just ENRFY and blank nanoparticles (100ug) with ENRFY, 5uM of free CHIR added to the media as a positive control, and 100ug of CHIR-loaded PLGA nanoparticles (PLGA-CHIR NPs) as the experimental group. PLGA-CHIR NPs and blank NPs were mixed in Matrigel and plated in wells adjacent to the spheroids-embedded Matrigel. This is

to create a ‘drug-depot’ effect so that the particles will not be removed during the media change. Culture plate was placed in the 5% CO_2 incubator at 37°C to allow polymerization of the Matrigel for about 15 minutes. After solidification, culture media was added and media was changed every two days. Similar procedure was followed for non-transduced spheroids, except that few additional conditions were included. Different conditions include: negative control well with spheroids cultured with just ENRFY and 2.5uM & 5uM of free CHIR were added to the media as positive control. Experimental wells had different amounts of CHIR-loaded PLGA nanoparticles (100ug, 200ug, 300ug) and blank nanoparticles (100ug). 100ug, 200ug and 300ug of nanoparticles were estimated to release about ~6uM, ~12uM and ~18uM of CHIR to the spheroids for a period of 7 days. The amount of CHIR loaded is about ~2ug per 100ug of the nanoparticles.

2.4.2 Small intestinal crypts

2.4.2.1 Isolation of crypts from the tissue

Crypts were harvested from the tissue according to the method proposed by Sato et al [27]. Briefly, a small incision is made on the proximal small intestine from the junction of the stomach and flushed with cold PBS until the luminal contents are flushed out. Villus is then scraped off the intestine and is cut into 2-4mm pieces using scissors. The fragments are further washed and vortexed gently for about 30 second in 3 second pulses and the supernatant is discarded. This step is repeated about 4-5 times until the supernatant is almost clear. 30mL of 2.5mM EDTA/PBS is added to the fragments and kept on a rocker for 30 minutes at 4°C. The fragments are allowed to settle down and supernatant containing EDTA is removed. Next, about 30mL of PBS is added to tissue fragments and vortexed gently for 30 seconds in 3 second pulses. Supernatant fractions are transferred to another tube to until the tissue settles down and this is

repeated until almost all of the crypts are released. Usually, majority of villi fragments are found in first and second fractions and mostly, the third to fifth supernatant fractions are enriched with crypts. Crypt fractions are then centrifuged at 100rcf for 2 minutes, supernatant is removed and resuspended in 10% FBS (100uL/mL of crypt fractions). After inspecting the fractions by inverted microscopy, it is filtered through 70-µm and 100-µm cell strainers (BD Biosciences) and then centrifuged at 100rcf for 2 minutes. The isolated crypt fragments are resuspended in 5mL of basic media composed of ADMEM/F12, GlutaMax, HEPES buffer and penicillin/streptomycin and centrifuged at 80rcf for 2 minutes to remove single cells. This procedure is repeated 2-3 times to wash off the single cells. Crypts are then stored at 4°C until further use.

2.4.2.2 Seeding Crypts

Isolated crypts are centrifuged briefly thrice for about 3 seconds to remove the supernatant and resuspended in Matrigel to a final concentration of 200 crypts/25uL of Matrigel. Crypts are seeded onto a 48-well culture plate. CHIR-loaded and blank nanoparticles are also plated adjacent to the crypts and rest of the procedure is followed similar to that of the spheroids. Here, culture media used is the same as the differentiation media described in spheroids section (2.4.1.1). Different culture conditions were employed for testing different concentrations of free CHIR and PLGA-CHIR NPs (50ug, 60ug, 70ug).

2.4.3 RNA Extraction and RT-qPCR analysis

RNA was extracted from cultured crypts according to the manufacturer's protocol (RNeasy Mini Kit; Qiagen). Quantitative real-time PCR was performed using 7500 Real Time Cycler (Applied Biosystems) on the total RNA extracted with QuantiTect Probe (Qiagen) with TaqMan gene expression (Life Technologies) to measure the expression levels of stem cells and differentiation

markers. Lgr5 and Olfm-4 were used as CBC stem cell markers and Alpi, Chga and Lyz as differentiation markers. RT-PCR was also done on RNA extracted from normal human intestine for normalization. The relative quantitative method ($2^{-\Delta\Delta Ct}$; Cycle times, Ct) method was used for quantifying target gene expression. Glyceraldehyde phosphate dehydrogenase (GAPDH) of normal small bowel was used as the reference gene to normalize the mRNA expression levels of other genes.

2.5 Data analysis and Statistical Significance

All of the in vitro results were expressed as the mean ± standard deviation of three replicates fr nanoparticles' characterization and two replicates for cell culture studies. Statistical analysis of the data was performed using unpaired Student's T-Test. A value of $p<0.05$ was used to determine statistical significance.

3. RESULTS

3.1 Determination of encapsulation efficiency and nanoparticle yield

Nanoparticles prepared by the single-emulsion/solvent evaporation method resulted in drug encapsulation efficiency of about 78.29±1.80 with the nanoparticle yield about 90% (mean ± std. dev., n=3. $p<0.05$).

3.2 Characterization of PLGA-CHIR Nanoparticles

Nanoparticles were characterized in terms of size and zeta potential. Size distribution and zeta potential measured for a sample is shown in Fig. 4(a) and (b). The size of the drug loaded and blank nanoparticles measured about 346.35±27.93nm and 403.75±13.08nm, respectively. Zeta potential of the drug-loaded and blank particles were about -34.25±7.70mV and -31.75±1.34mV, respectively (mean ± std. dev., n=3, $p<0.05$).

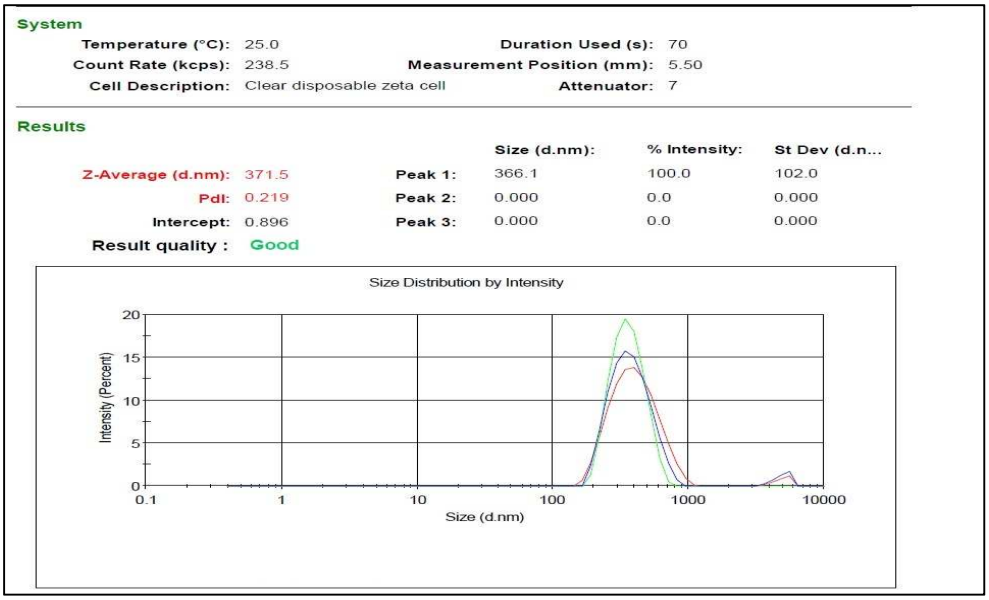

Figure 4. (a) Size distribution of PLGA-CHIR Nanoparticles

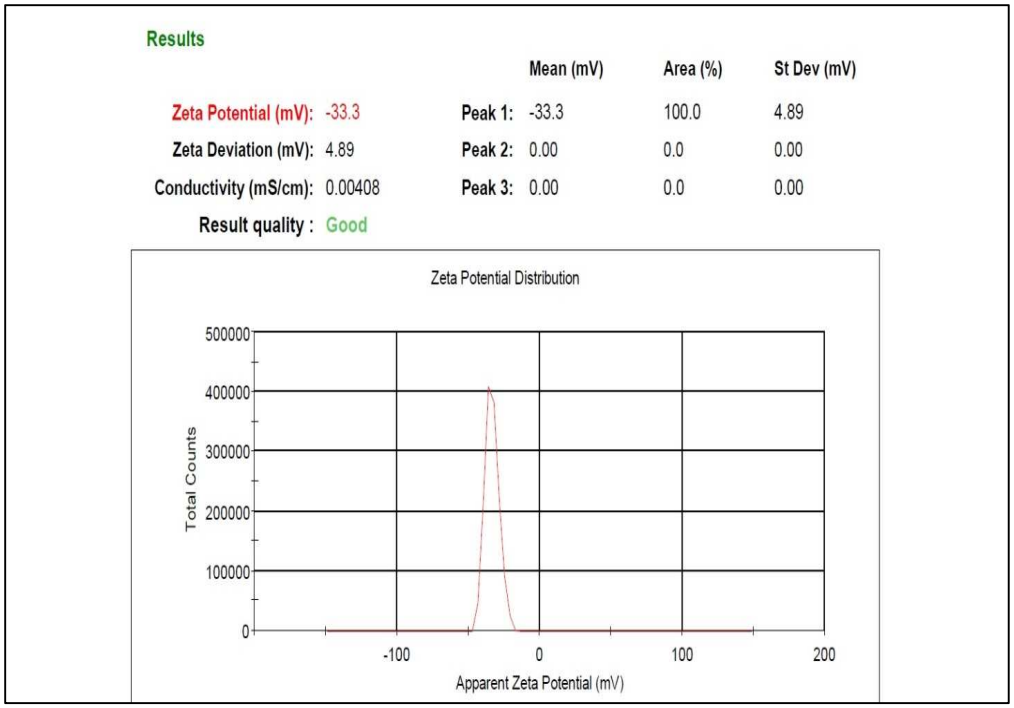

Figure. 4 (b) Zeta potential of PLGA-CHIR Nanoparticles

The formulation factors with the characteristics features of the fabricated nanoparticles are tabulated in Table 1.

	Ultrasonication time	Size, nm	Polydispersity Index	Zeta potential	Drug Loading	Encapsulation Efficiency %
CHIR-loaded PLGA nanoparticles	50 seconds	346.35±27.93	0.32±0.05	-34.25±7.7	2%	78.29±1.8%
Blank Nanoparticles	50 seconds	403.75±13.08	0.29±0.07	-31.75±1.3	—	—

Table 1. Physicochemical characteristics of drug-loaded and blank PLGA nanoparticles (mean ± std. dev., n=3. $p<0.05$)

3.3 Scanning Electron Microscopy

Scanning electron microscopy (SEM) analysis of PLGA nanoparticles was performed at 10,000X magnification. The surfaces appeared smooth and spherical in shape with their size ranging from 350nm to 420nm (Fig.5).

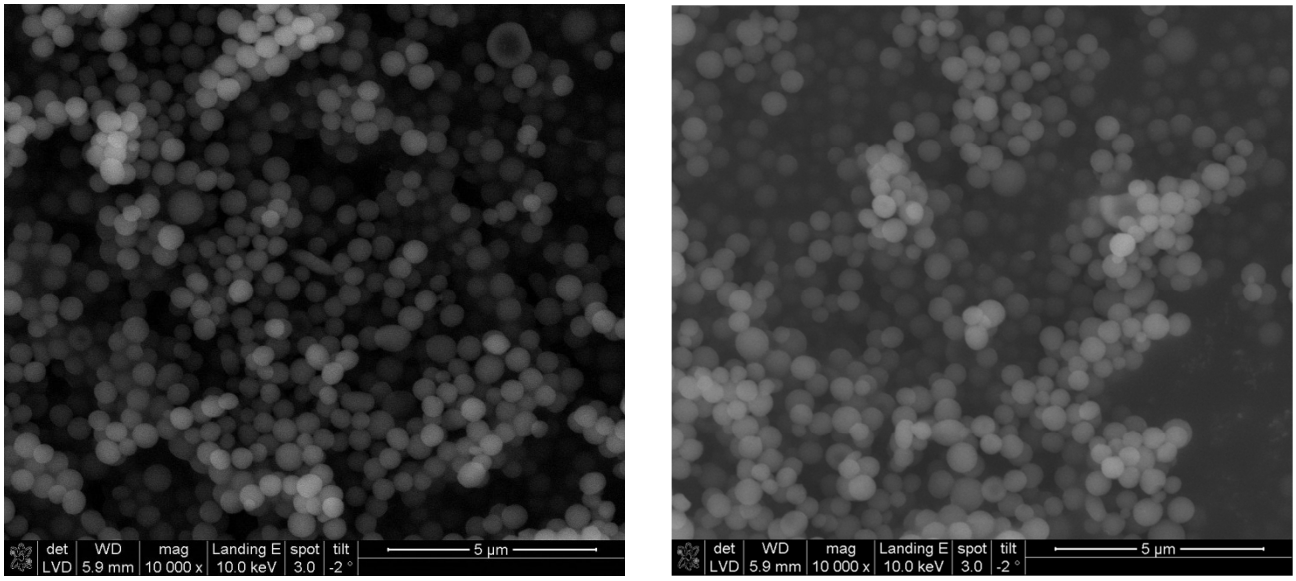

Figure 5. SEM image of (A) Blank PLGA Nanoparticles (B) PLGA-CHIR Nanoparticles

3.4 In vitro release study

The in vitro release study of CHIR-loaded nanoparticles was determined in 0.01M PBS at 37°C. The cumulative CHIR release percentage is shown in Fig. 6(c). After the initial burst release of about 50% for about 24 hours, the release rate of CHIR gradually decreased and followed almost zero-order release kinetics. The initial burst release is the characteristic feature of drug

encapsulated micro/nanoparticles. Burst release during the first few hours might be due to the dissolution and diffusion of the drug closer to the surface of the nanoparticles compared with those drug molecules entrapped within the polymer matrix which accounts for the slower, steady release. The standard profile of CHIR99021 determined by UV spectroscopy is shown in Fig. 6(a) & 3(b). CHIR has its maximum wavelength absorbance at 282nm.

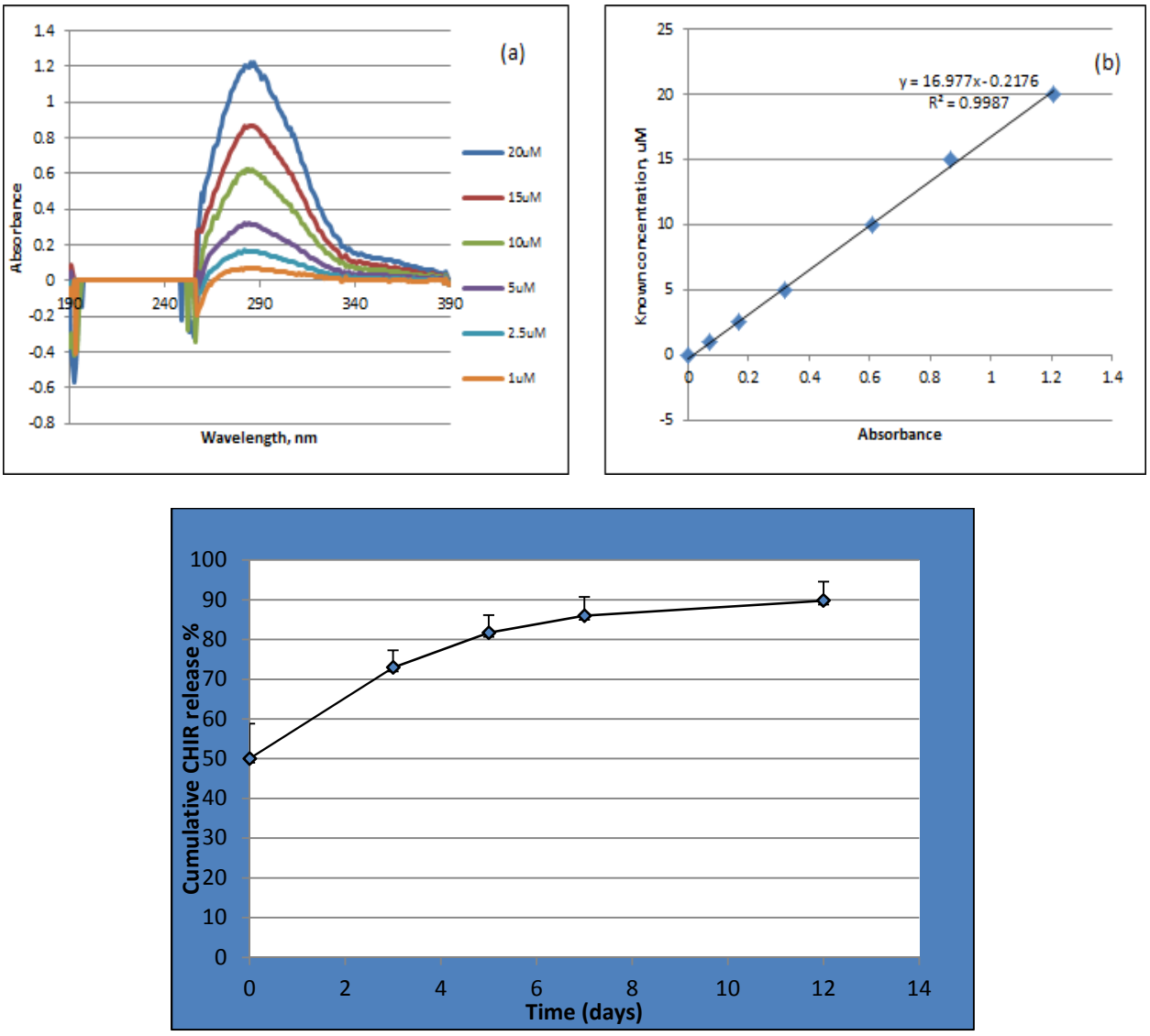

Figure 6. Characteristic profile of CHIR99021 (a) Standard profile, (b) Standard concentration vs absorbance curve & (c) Cumulative CHIR release from PLGA nanoparticles (mean ± std. dev., n=3. $p<0.05$)

3.5 In vitro cell culture study

3.5.1 Lenti TCF/LEF reporter transduced spheroids

In order to demonstrate that CHIR99021 acts by triggering the Wnt/ β-catenin pathway, a promoter reporter assay was conducted using the β-catenin-dependent TOP-FLASH reporter plasmid. Different culture conditions were used in the experimental wells to prove fluorescent-related Wnt signaling in the small intestinal spheroids. As a negative control, spheroids were cultured with basic media and growth factors constituting EGF, Noggin, R-spondin1, FGF-10 and Y-27632 (ENRFY). CHIR (5uM) was added to the spheroids along with the ENRFY media as positive control. The experimental culture wells had ENRFY media with PLGA-CHIR NPs (~100uG) embedded in Matrigel to match CHIR concentration in positive control wells and blank PLGA NPs to match the negative control. Figure 7(A) shows culture day 0 as a sample panel of spheroids just before adding the differentiation media. Morphologically, in the first 48-72 hours, spheroids culture with CHIR (free and encapsulated forms) started shrinking in size compared with those that didn't receive CHIR and few spheroids started to fluoresce already denoting the activation of Wnt/βcatenin signaling. By culture day 7, the number of fluorescing spheroids increased significantly with PLGA-CHIR NPs (Fig. 7D) evidencing the release of CHIR from the NPs with results comparable to that of the positive control wells (Fig. 7C). On the other hand, the wells with just the culture media didn't exhibit much fluorescence (Fig. 7B&E) although very few spheroids fluoresced (image not shown). This could be because the culture media has growth factors to support survival of the cells for a few days and there could be other signaling processes along with Wnt going on in their metabolism. Wnt agonist R-Spondin1 in the media could possibly help enhance Wnt signaling in the spheroids to some extent although it is not as predominant as in the case of those that received CHIR, since R-spondin-1 is only a Wnt enhancer in the presence of other Wnt activating factors.

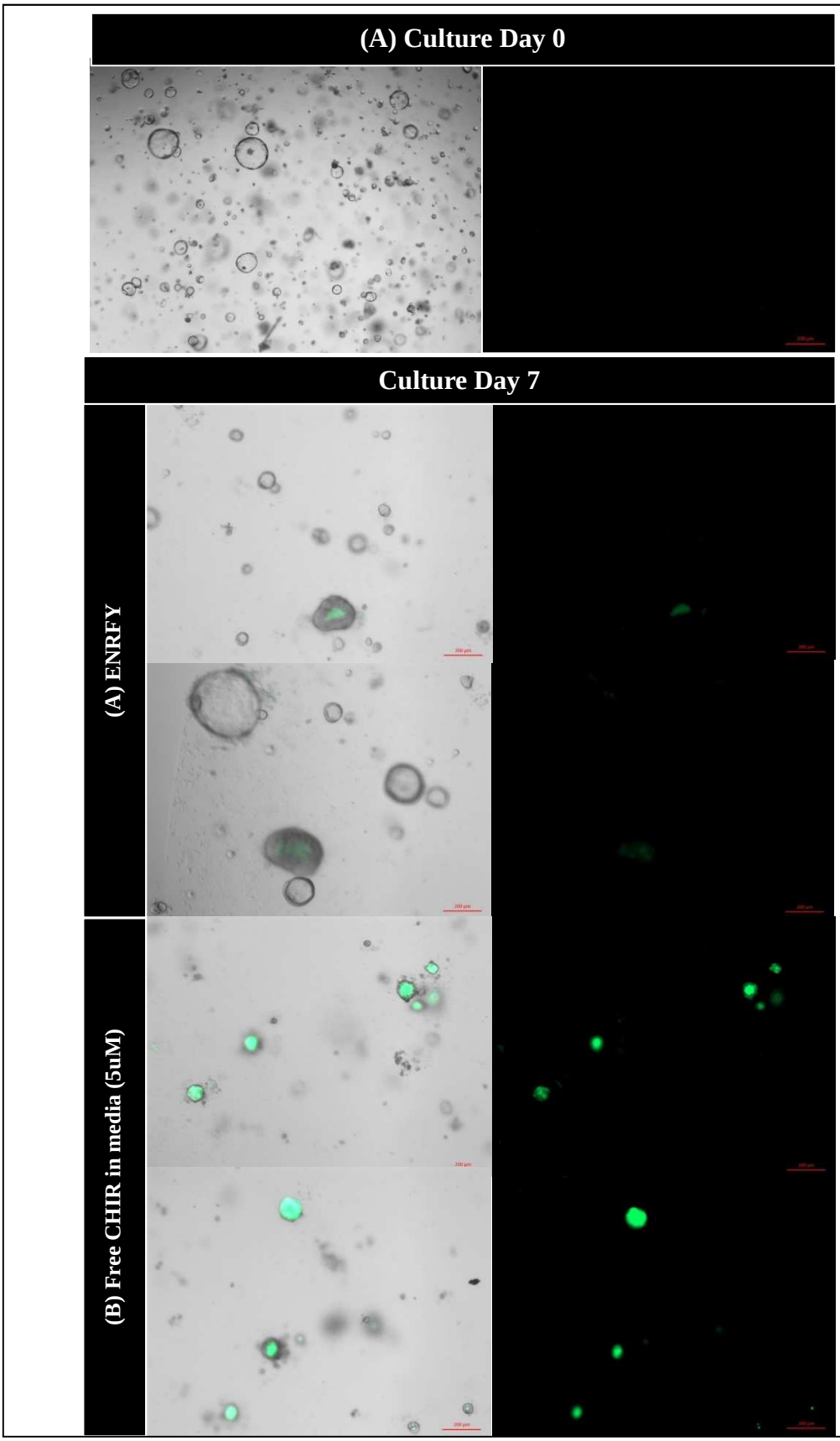
(A) Culture Day 0
Culture Day 7
(A) ENRFY
(B) Free CHIR in media (5uM)

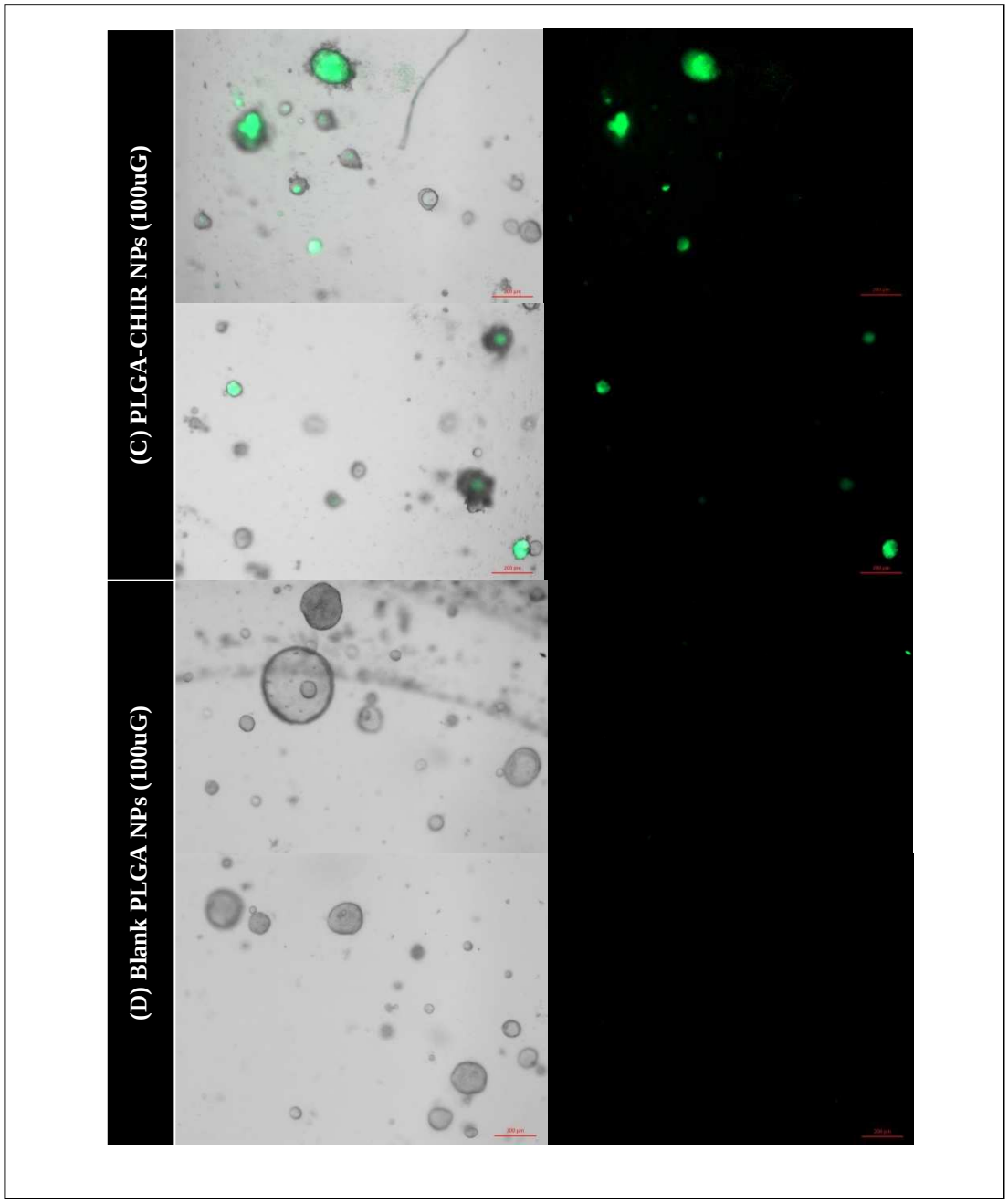

Figure 7. PLGA-CHIR Nanoparticles' Efficacy on lentiviral transduced TOP/GFP reporter in the human small intestinal spheroids. Images show culture day 6 results. Panel (A) Spheroids on culture day 0. Panel (B) Negative control, ENRFY media without CHIR: no fluorescence (green) spheroids in shows less or no Wnt signaling. Panel (C) Positive control, free CHIR (5uM) in media shows enhanced fluorescence in many spheroids. Panel (D) CHIR encapsulated in PLGA NPs (100uG) shows fluorescence in spheroids similar to 5uM wells. Panel (E) Blank PLGA NPs similar to that of negative control wells showing no fluorescence. Scalebar, 200uM. Left and right panel shows brightfield and fluorescent images, respectively.

Scale bar, ——200um.

3.5.2. Non-transduced spheroids

In the next set up, PLGA-CHIR nanoparticles were tested on non-transduced spheroids in order to determine the growth/developmental changes induced by CHIR on the spheroids, as other than fluorescence not much significant morphological growth was observed on lenti TCF/LEF reporter transduced spheroids. Culture conditions and media were established similar to lentiviral transduced spheroids. Fig. 8A shows a sample panel of spheroids on the day just before adding the differentiation media (4 days after passaged spheroids were cultured in myofibroblasts conditioned media). Culture day 7 images are shown in Figs. B through H. As shown, spheroids that received no CHIR but cultured with just ENRFY (Fig. 8B) and blank PLGA NPs (Fig. 8H), mostly remained as spheroids with very few of them being in the trans state of becoming enteroids, although did not completely convert to enteroids, for the same reason as explained in the case of lentiviral transduced spheroids. But those that received CHIR - free CHIR (Figs. 8C&D) and PLGA-CHIR NPs (Figs. E,F&G) - clearly showed morphological transformation where most of the spheroids were converted to enteroids with more complex structures and others were found as enterospheres which would later convert to enteroids if culture days are prolonged.

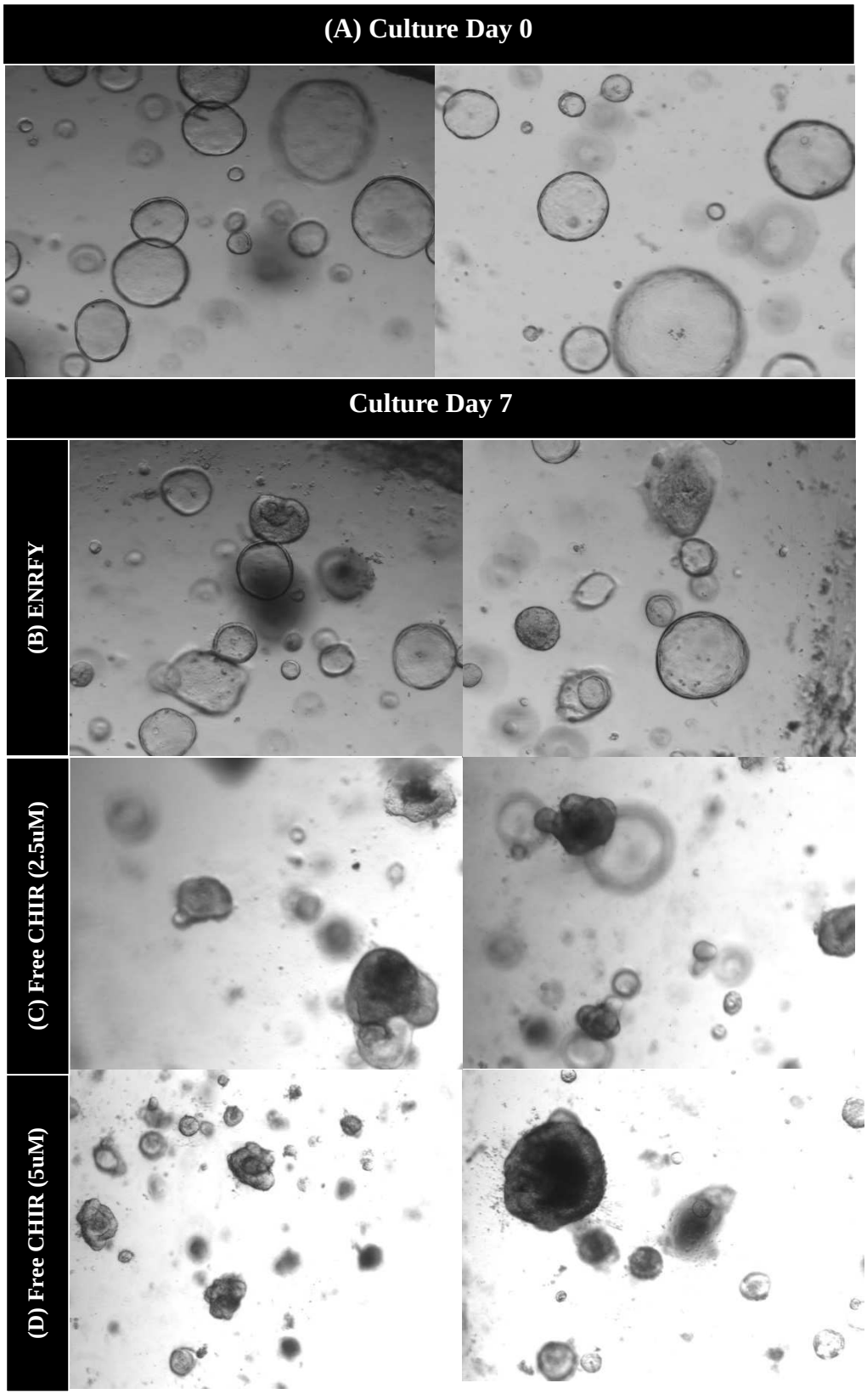
(A) Culture Day 0
Culture Day 7
(B) ENRFY
(C) Free CHIR (2.5uM)
(D) Free CHIR (5uM)

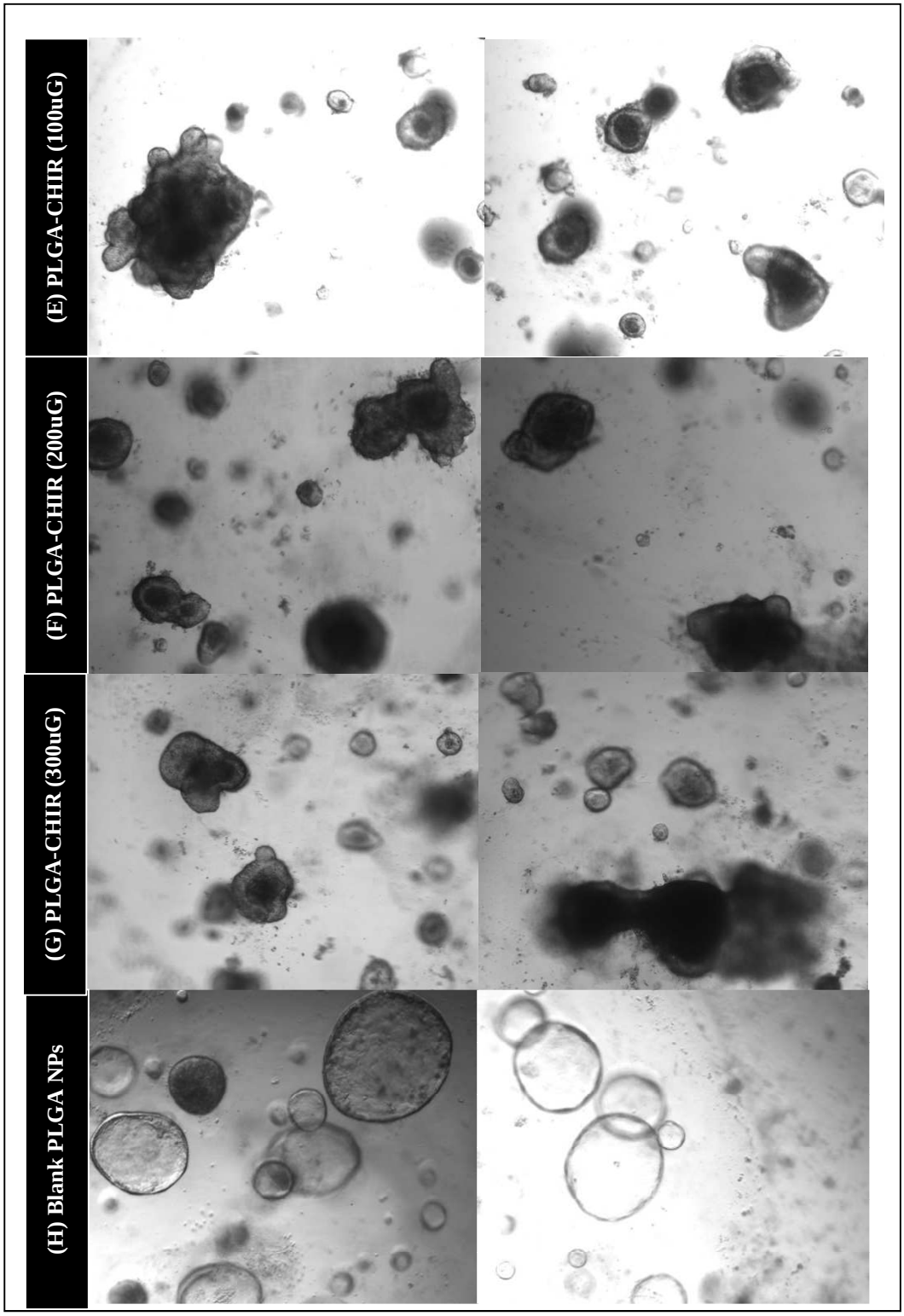

Figure 8. Efficacacy of PLGA-CHIR nanoparticles on non-transduced adult human intestinal spheroids. Panel (A) Spheroids passaged and cultured for 4 days: just before adding the differentiation media, used as a representative of all other wells. Culture day 7 results: Panel (B) Negative control: spheroids in ENRFY media. Panel (C&D) Free CHIR (2.5uM & 5uM respectively). Panel (E, F & G) PLGA-CHIR NPs (100uG, 200uG & 300uG respectively) . Panel (H) Blank PLGA NPs. Scale bar ____200um.

3.5.3. Small Intestinal Crypts

Similar experiment was conducted on small intestinal human crypts with experimental settings similar to that of spheroids. Culture medium comprises of basic ADMEM/F12 media with HEPES buffer, penicillin/streptomycin, Glutamax, N2, B27, NAC and growth factors include EGF, Noggin, R-Spondin1, FGF-10 and Y-inhibitor (concentration was maintained similar to previous experiments). In this culture assay, experimental conditions were employed to determine both the morphological and molecular level changes in crypts induced by CHIR. Culture day 4 images are shown in Fig. 9. Here, lesser amounts of nanoparticles were used unlike spheroids, about ~50uG to 70uG were used in experimental wells. This is because previous experimental results showed that higher concentrations of CHIR didn't support proper growth/development of crypts and that the developing crypts seemed to die off during the first few days of culture. As seen in Fig.9A, crypts grown with just the culture media (ENRFY) without CHIR formed cystic enteroids without budding whereas crypts that were grown with free CHIR in the media, 2.5uM (Fig.9B) and 5uM (Fig.9C) seemed to develop into elongated and irregular shaped enteroids with structures more inclined to developing budding structures as early as in the first few days. Similarly, the experimental wells with increasing amounts of CHIR (Fig. 9D through 9F, 50uG, 60uG & 70uG) also showed comparable results as that of free CHIR wells whereas the crypts cultured with blank nanoparticles (Fig. 9G) exhibited cystic growth without any budding, suggesting that not much complex growth was supported.

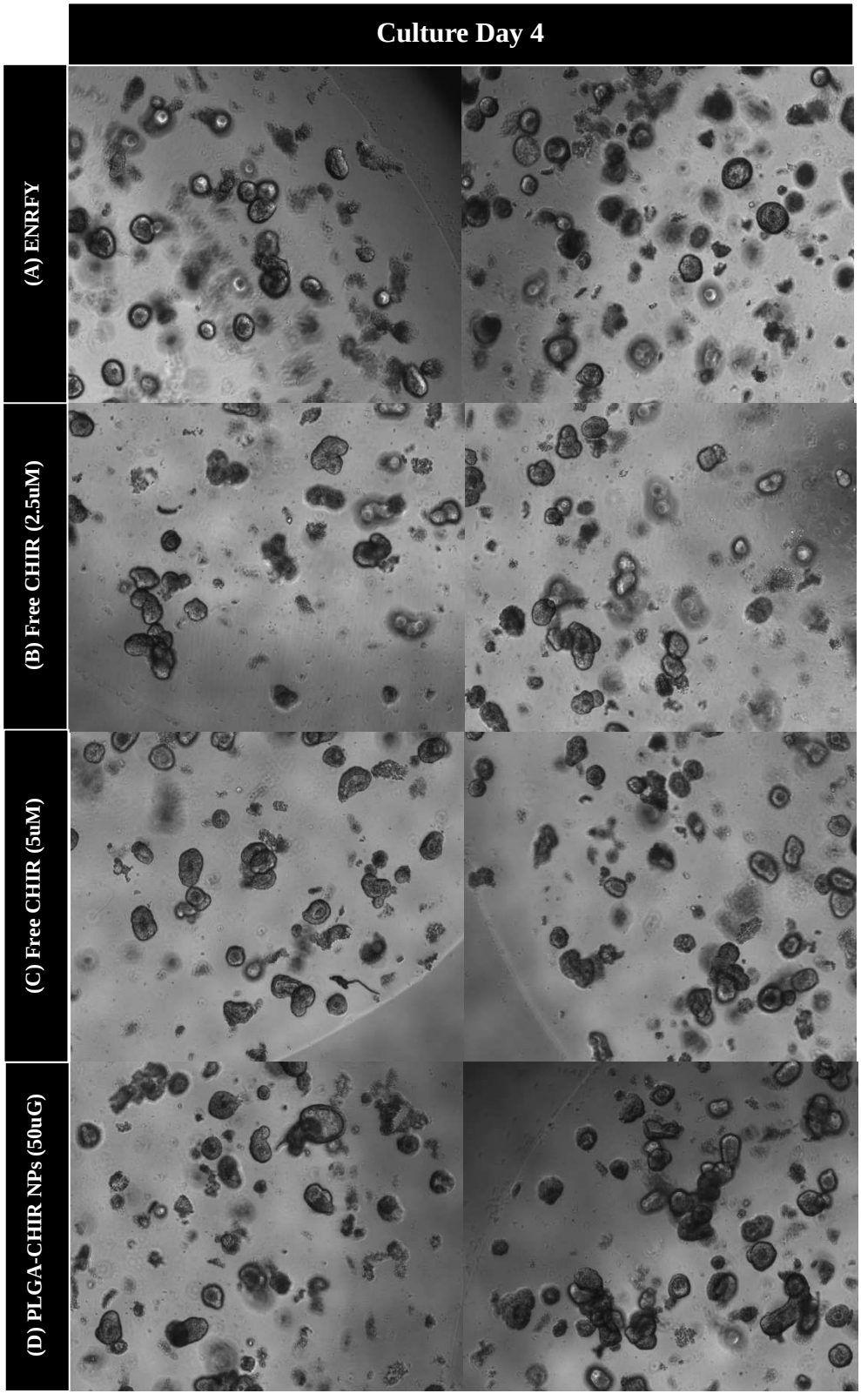
Culture Day 4
(A) ENRFY
(B) Free CHIR (2.5uM)
(C) Free CHIR (5uM)
(D) PLGA-CHIR NPs (50uG)

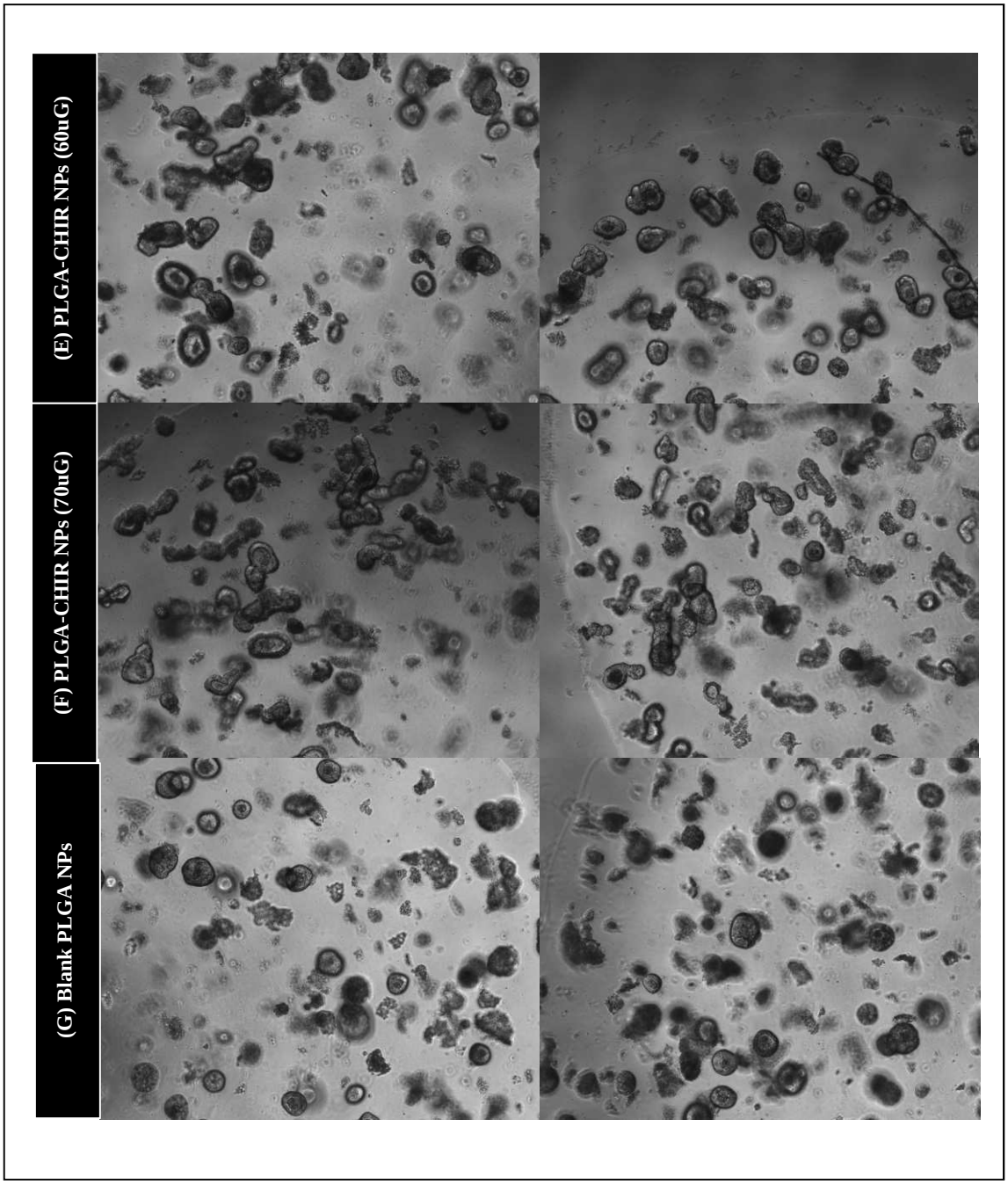

Figure 9. PLGA-CHIR nanoparticles' induced effect on isolated human small intestinal crypts. Culture day 4. Panel (A) Negative control group: ENRFY without CHIR. Panel (B&C) Positive control group: Free CHIR (2.5uM & 5uM respectively). Panel (E, F, G & H) Experimental group: PLGA-CHIR NPs (E) 50uG, (F) 60uG, (G) 70uG) & (H) Blank PLGA NPs respectively. Scale bar ——200um.

Figure 10.
CHIR99021's ability to promote survival by regulating anti-apoptotic/survival pathways in human small intestinal crypts. Crypt cultured without ROCK inhibitor (Y-27632), culture day 7.
Panel (A) Negative control group: ENRF without CHIR.
Panel (B&C) Positive control group: Free CHIR (2.5uM & 5uM respectively).
Panel (D) PLGA-CHIR NPs (50ug).
Panel (E) Blank PLGA NPs.
Scale bar —— 200um.

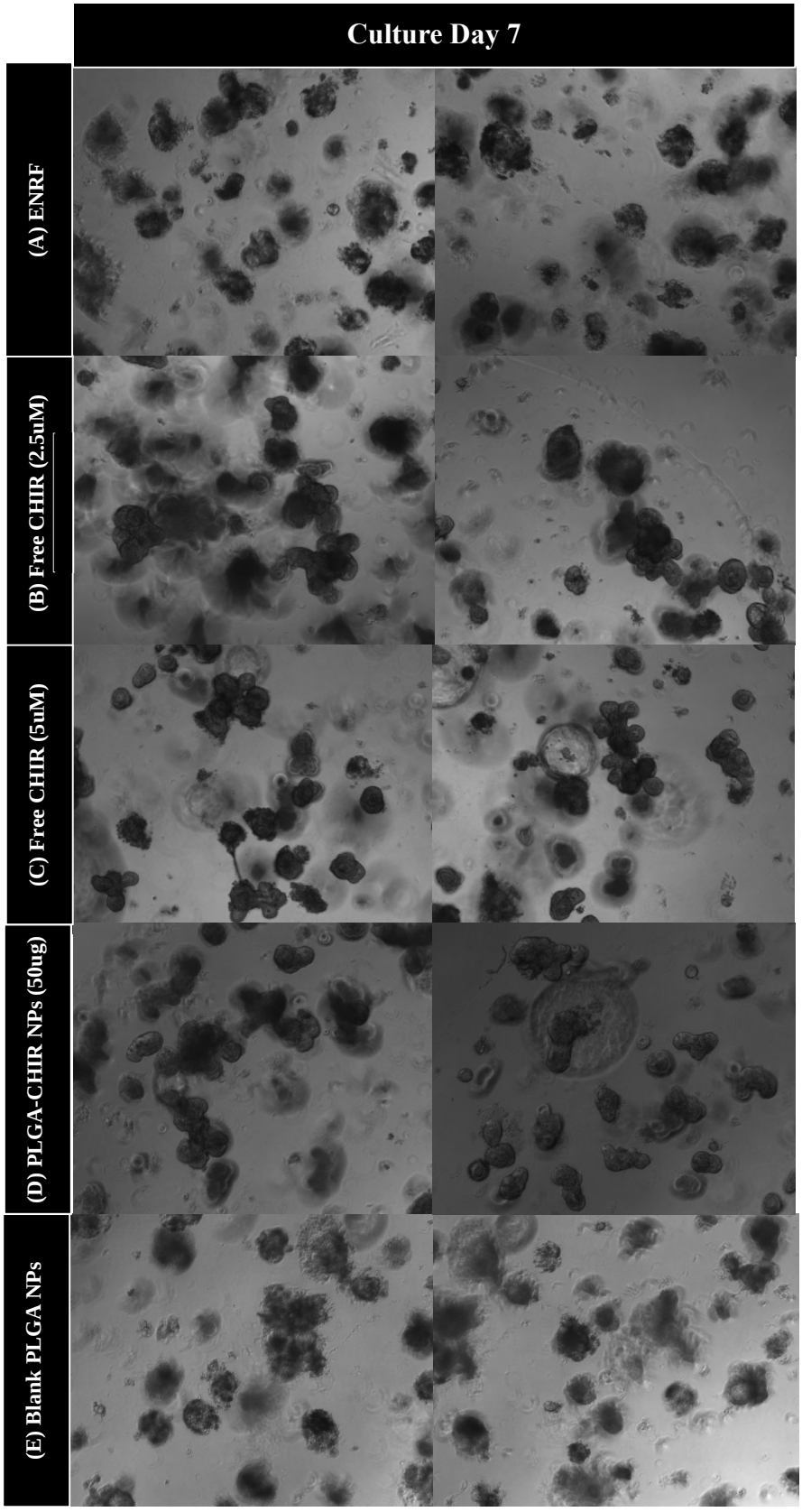

Another cell culture experiment was conducted to analyze CHIR's ability to regulate cell survival and anti-apoptotic pathways in small intestinal crypts. In this particular experiment, crypts were cultured without ROCK inhibitor, Y-27632 throughout the culture days. As seen in Fig. 10A & B, the crypts did not survive by culture day 7 whereas crypts treated with 2.5uM and 5uM CHIR, the positive control group survived with more complex morphology. Likewise, the experimental crypts with 50ug of PLGA-CHIR NPs survived exhibiting similar phenomena as that of the free CHIR control group, once again proving that the pharmacological activity of inhibitor encapsulated PLGA nanoparticles is intact.

3.5.4 RT-qPCR Results

Quantitative real-time PCR analysis was performed on crypts cultured for 4 days under conditions as described earlier for evaluating relative mRNA expression of intestinal epithelial stem cell and differentiated cell markers. *Lgr5+* and *Olfm4* are the markers for CBC intestinal stem cells. *Alpi*, *Chga* and *Lyz* are the differentiated cell markers of enterocytes, enteroendocrine cells and Paneth cells, respectively. As shown in Fig. 11A, with increasing doses of CHIR, increasing *Lgr5* gene expression was observed. The highest free CHIR 5uM had about 30-fold increase in *Lgr5* gene expression compared with crypts cultured with just ENRFY and blank NPs. This is comparable with the experimental group, 70ug of PLGA-CHIR NPs, which had about 27-fold increase. And, 2.5uM CHIR, 50ug and 60ug PLGA NPs had about 3-fold, 10-fold and 20-fold increase in *Lgr5* gene expression, respectively. About 2 to 4-fold increase was observed in *Olfm4* gene expression. Further, 5uM and 70ug PLGA-CHIR CHIR-treated crypts had about 15-fold and 11-fold decrease in enterocytes' mRNA expression (*Alpi*), so does the enteroendocrine mRNA expression (*Chga*) which showed about 3-fold increase throughout.

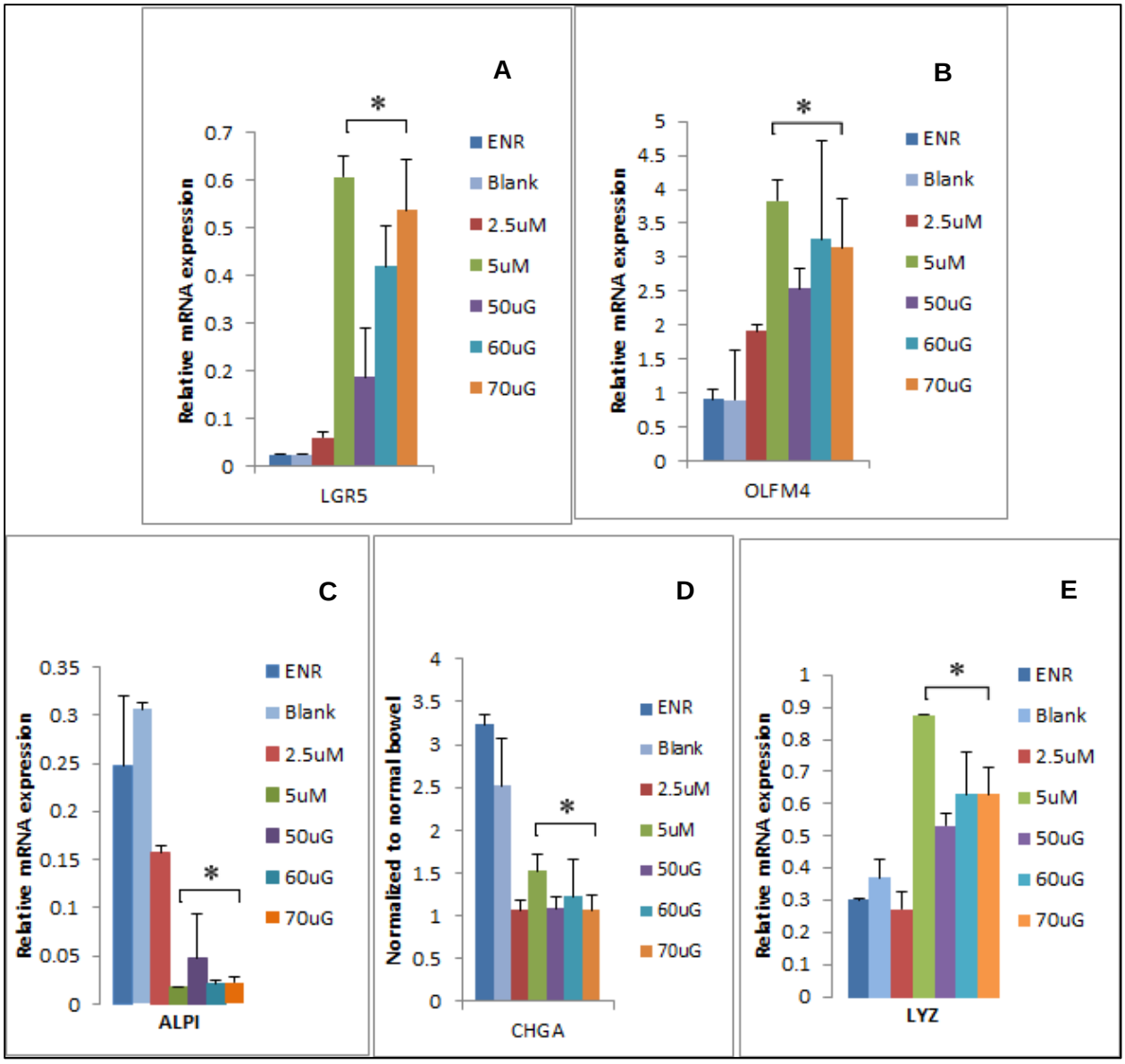

Figure 11. Quantitative real-time PCR analysis (qRT-PCR) of normalized mRNA expression of stem cell and differentiation markers for intestinal epithelial cells (A) *Lgr5* and (B) *Olfm4* for CBC ISCs, (C) *Alpi* for enterocytes, (D) *Chga* for enteroendocrine cells, (E) *Lyz* for Paneth cells cultured for 4 days under conditions as indicated. Error bars, s.d. (mean ± std. dev., n=2. statistical significance maintained between positive control, 5uM and 50ug to 70ug PLGA-CHIR NPs (*p<0.05))

4. DISCUSSION

The identification of intestinal stem cell marker, Lgr5 is a major breakthrough in the field of small intestinal tissue engineering and gene therapy. Recent demonstrations about the ability to develop ‘mini guts’ from the Lgr5 stem cells has facilitated efforts to tissue engineer small intestine ex vivo, channelizing it toward a completely functional organ for transplantation in vivo.

During small intestinal organogenesis, there are various molecular signaling processes, including Wnt, Notch, BMP, Hedgehog, and feedback/crosstalk mechanisms between them that orchestrate to develop multiple cell types into a functional tissue/organ. Of all the above, Wnt signaling has been established to control/maintain self-renewal of the stem cells in the small intestinal tissue. A small molecule GSK-3β inhibitor, CHIR99021 (CHIR) has been identified to target specifically Wnt signaling pathway to induce self-renewal and proliferation of Lgr5+ stem cells residing in crypts. Though, this small molecule inhibitor has extensively been used in vitro, not many efforts has been taken to translate this effect in vivo. Hence this study, in an attempt to take this to a next level, intended to utilize bioengineering approaches to effectively translate these effects in vivo. As mentioned earlier, about the many advantages of shielding a drug to avoid being destroyed before realizing its efficacy in vivo, the small molecule drug was encapsulated using nanoparticles made up of PLGA, an approved polymer that is both biocompatible and biodegradable. In this study, PLGA NPs were prepared by a technique called single-emulsion/solvent evaporation method. PLGA crystals were dissolved in a water immiscible solvent, dichloromethane along with the drug solution. This constitutes the organic phase. Poly vinyl alcohol and sodium dodecyl sulfate were used as emulsifier and stabilizer of nanoparticles. Resultant nanoparticles were in a size range of about 350nm – 400nm. Zeta

potential was in the range from -31mV to -34mV. Zeta potential is the measure of stability of any colloidal dispersion. Higher the zeta potential, lower the aggregation, more is the stability of the nanoparticles. Zeta potential of about -33mV implies that the particles are stable and less likely to aggregate. The drug encapsulation efficiency was about 78% to 80% with nanoparticle yield about 90%. Increasing the organic to aqueous phase ratio from 1:16 to 1:8 resulted in particle size range transformation from micrometer to nanometer sized particles and also helped increase encapsulation efficiency (Table 1). The in vitro release showed a biphasic release profile with an initial burst release of about 50% followed by a slower release phase (Fig. 6c). PLGA degrades via hydrolysis due to breaking of ester linkages in aqueous environments and encapsulated drug is slowly released due to degradation but also might occur due to diffusion and swelling of the polymer matrix. Since the degradation of PLGA is really slow for polymers of high molecular weight, release of CHIR (being a small molecule) would depend predominately on diffusion or at least during the time of experimental studies. In order to test the efficacy of the nanoparticle-encapsulated CHIR, four in vitro cell culture studies were performed. In all these cases, the nanoparticles were mixed in Matrigel and plated in wells adjacent to the spheroids- and crypts-embedded Matrigel so as to create a 'drug-depot' effect and that the particles will not be removed during the media change (Fig. 12).

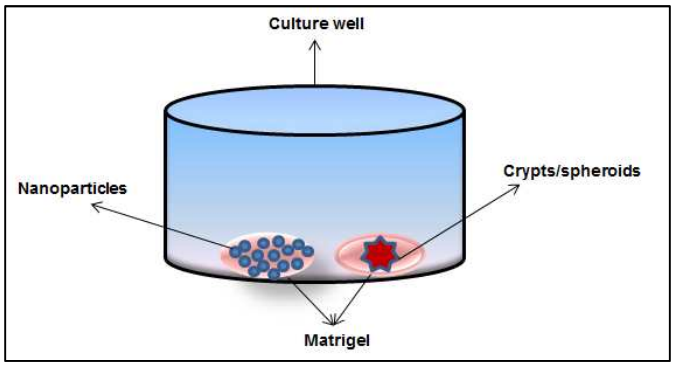

Figure 12. Culture well setup

First, in order to demonstrate that CHIR activates canonical Wnt signaling, PLGA-CHIR were tested on lenti TCF/LEF reporter transduced spheroids. This reporter assay employs transduction of cells with lentiviral particles with TCF/LEF reporter expressing green fluorescent protein (GFP) gene which is used as a measure for monitoring the canonical Wnt signaling activity (mechanism of action is illustrated in Fig. 13). Upon activation of Wnt signaling by CHIR99021, β-catenin translocates to the nucleus and binds to the TCF/LEF transcription factors which in turn activate Wnt target genes. In this case, the nuclear translocated β-catenin binds to TCF/LEF reporter which is programmed to activate genes for transcribing GFP which then causes the epithelial cells to emit fluorescence. Lenti viral-transduced spheroids were cultured in basic culture media with growth factors ENRFY for a total of about 7 days after adding the differentiation media. The experimental set up comprises of spheroids cultured with and without CHIR (free in media and PLGA encapsulated CHIR). As shown (Fig. 7), after culturing them for about 7 days, spheroids with PLGA-CHIR nanoparticles (NPs) were relatively smaller in size and others were in the trans-state of converting to enteroids (Fig. 7C), similar to the control group which received free CHIR, 5uM (Fig. 7B). Moreover, many spheroids fluoresced brightly compared with those that were cultured without CHIR (ENRFY (Fig. 7A), Blank NPs (Fig. 7D),) which remained relatively bigger in size with less or no fluorescence. This observation confirmed CHIR released from nanoparticles is biologically active and that it stimulated Wnt/β-catenin activity.

Secondly, a similar experiment was conducted on non-transduced human small intestinal spheroids in order to evaluate the morphological changes induced by CHIR on these cells since not much morphological transformation was observed on viral-transduced spheroids, as Wnt signaling-derived effects were intercepted by lentivirus with TCF/LEF reporters. The culture

conditions were similar to the former experiment except that different concentrations of CHIR (free and encapsulated forms) were tested on these spheroids.

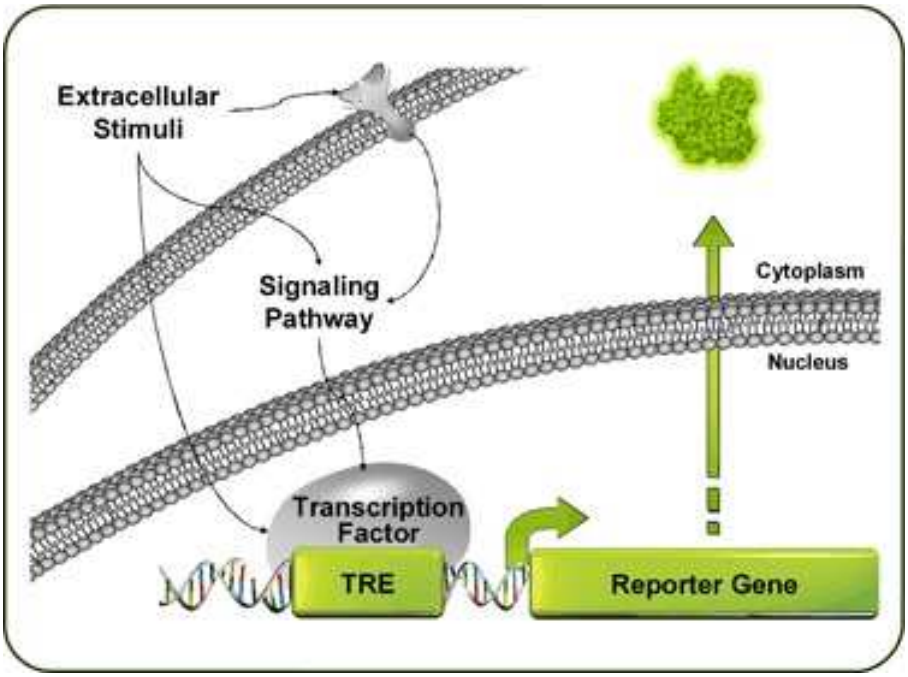

Figure 13. TCF/LEF reporter's mechanism of action during Wnt signaling

(http://www.sabiosciences.com/reporter_assay_product/HTML/CLS-018G.htm)

As shown (Fig. C through G), the spheroids with CHIR first reduced in size, then gradually started forming double-walled structures and started gaining irregular structures. Eventually they converted to mature enteroids more towards developing full-fledged organoids. Many enteroids developed complex morphology as seen by the developing buds with a lot of debris in the lumen. Whereas ENRFY and blank NPs group with no CHIR mostly remained as spheroids (Fig. 8B&H). Once again, CHIR99021's activity is confirmed that it triggers canonical Wnt signaling in spheroids to convert them into enteroids which in the presence of other growth factors/inhibitors like nicotinamide, gastrin, TGF-β and p38 inhibitor in the culture media will develop more complex structures that express function intestinal epithelial units.

Finally, the PLGA encapsulated CHIR nanoparticles were tested on human small intestinal crypts harvested from small intestinal tissue. This was to determine the molecular level changes induced by CHIR by triggering Wnt pathway and that the small molecule is capable of stimulating proliferation of Lgr5+ CBC stem cells. During the recent years, research studies reported that CHIR is capable of maintaining pluripotency in human and mouse embryonic stem cells (mESCs) by activating Wnt signaling [35]. But, a most recent study reported that, CHIR not only promotes Wnt signaling, but also altered various other pathways such as MAPK, TGFβ and Notch signaling pathways in mESCs. Moreover, transcription factors responsible for maintaining pluripotency were up-regulated while other developmental genes were down-regulated. But this is just with mESCs and there could be myriad of other signaling pathways/ transcription factors that could be regulated in adult human intestinal cells that warrant much research, as its downstream effects are not yet completely studied [51]. Here again, the experimental set up was similar to previous conditions. As early as 4 days in culture, significant difference was observed both morphologically and molecularly (RT-PCR results). Crypts grown in basic media with just the growth factors EGF, Noggin, R-spondin1, FGF-10 and ROCK inhibitor formed mostly cystic enteroids (Fig.9A) whereas the crypts cultured with CHIR (2.5uM and 5uM, Fig. 9B & C) formed elongated, irregular-shaped enteroids with small protrusions which later would possibly develop into budding structures. Also, crypts cultured with 50ug to 70ug of PLGA-CHIR NPs showed similar morphology (Fig. 9D-9F) as that of the 2.5uM and 5uM free CHIR control group. In another independent experiment, CHIR was also tested on these crypts with all similar conditions but without including inhibitor of Rho-associated, coiled-coil containing protein kinase (ROCK) pathway, Y-27632. This small molecule has been reported to enhance survival of human embryonic stem cells (hES) by preventing apoptosis

during isolation of single cells [47] and also has been found to improve survival rates of hES during freeze-thaw process [48]. It was observed that the crypts with just ENRF media began to die off by culture day 3 or 4 and completely died after a week while those that received CHIR (both free and PLGA encapsulated CHIR) managed to survive with complex morphology (Fig. 10). In all the 4 cases, the morphological changes brought forth by this small molecule inhibitor are demonstrated well. In addition, the benefit of administering CHIR to these crypts was further strengthened by the fact that it helped achieve proliferation of Lgr5+ stem cells as shown by the gene-expression profiling of quantitative PCR measurement results (Fig. 11). Based on the mRNA expression, it was observed that crypts grown with just the ENRFY media and blank NPs had the lowest expression of *Lgr5* and *Olfm4* genes, the stem cell markers of CBC cells. But crypts treated with CHIR of concentrations, 2.5uM, 5uM and NPs of about 50ug, 60ug and 70ug had about at least 3, 30, 10, 20 and 27 folds higher expression of Lgr5 (Fig. 11A), respectively. In the same order, Olfm4 was about 2 to 4 folds higher for free CHIR control group and experimental PLGA-CHIR NPs group (Fig. 11B). Further, crypts treated with CHIR had reduced expression of enterocytes (marked by alkaline phosphatase, *Alpi*, Fig. 11C) and enteroendocrine cells (marked by Chromogranin, *Chga*, Fig. 11D) but increased expression of Paneth cells (marked by lysozyme, *Lyz*, Fig. 11E). This particular result where increased Lysozyme expression was observed with addition of CHIR has been previously reported in mice intestinal epithelial cells [49]. Though, Paneth cells are terminally differentiated cells, unlike other epithelial cells, they do not move up on the villus, rather reside at the bottom of the crypts adjacent to stem cells. Paneth cells are crucial for supporting Lgr5+ stem cells, since they not only secrete anti-micrbial peptides but also provide essential niche signals, *Wnt* and *Notch* [50]. They secrete Wnt3, EGF, noggin and DLL4 which are niche essential factors. Hence, increase in

Paneth cells' expression *Lyz* alongside *Lgr5* is another welcoming effect as a result of a treatment with CHIR. While CHIR released from PLGA NPs had expression of all genes at least equivalent to 5uM concentration or had a dose-dependent expression of genes, CHIR of 2.5uM was observed to be on the lower end of the spectrum. At the same time, it was ensured that the increasing amounts of PLGA-CHIR NPs did not exceed the cytotoxicity levels. This study, thus, once again proves CHIR99021 encapsulated in PLGA nanoparticles has preserved biological activity and targets Wnt/β-catenin signaling pathway which regulates growth, development and proliferation of small intestinal CBC epithelial stem cells by controlling their differentiation.

5. CONCLUSIONS & FUTURE DIRECTIONS

The identification of a GSK-3β inhibitor, CHIR99021 has led to the realization of sustaining Lgr5+ ISCs and long-term culture and expansion of small intestinal epithelial cells ex vivo. Isolated crypts containing Lgr5+ intestinal stem cells cultured in 3D environment are capable of developing into multicellular organoids that are a miniature version of a normal gut resembling closely to their in vivo counterparts. Though the small molecule's effect has been realized in vitro, not much efforts are taken to translate this effect in vivo. Hence, this study proposed an approach to realize the small molecule drug induced effect in vivo. In order to do so, CHIR99021 was appropriately encapsulated using PLGA nanoparticles, with manageable physicochemical properties and controlled drug release profile. Various cell culture assays to test the activity of encapsulated CHIR99021 demonstrated its efficacy by activating and regulating various signaling cascades, especially Wnt/β-catenin activity which is a critical regulating pathway of small intestinal stem cells. This study has elucidated the effect of CHIR99021 in a dose-dependent manner on small intestinal epithelial cell types with its striking preservation of pharmacological activity. Thus, this bioengineering-guided approach to intestinal organogenesis could possibly help channelize CHIR99021-induced effect for regenerative applications. In future, other potent molecules that support in vivo tissue regeneration could possibly be encapsulated along with CHIR99021 and could be loaded onto a scaffold for in situ delivery adjacent to ex vivo developed epithelial units, thus creating a 'drug cocktail depot' for small intestinal tissue transplantation and regeneration. Advances in the field of biology, regenerative medicine combined with bioengineering approaches thus opens up a promising venue for engineering small intestinal tissue as an 'elixir' to various intestinal abnormalities.

6. REFERENCES

1. Stollman NH, Neustater BR, Rogers AI. Short bowel syndrome. *Gastroenterologist* 4:118-128 **(1996)**

2. Buchman AL. Etiology and Initial Management of Short Bowel Syndrome. *Gasteroenterology* 130: 5-15 **(2006)**

3. Walter C. Faubion, John R. Wesley, Nabil Khalidi & Joseph Silva. Total Parenteral Nutrition Catheter Sepsis: Impact of the Team Approach. *Journal of Parenteral and Enteral Nutrition* 10: 642-645 **(1986)**

4. B Peyret, S Collardeau, S Touzet, I Loras-Duclaux, H Yantren, M C Michalski, J Chaix, L Restier-Miron, R Bouvier, A Lachaux and N Peretti. Prevalence of liver complications in children receiving long-term parenteral nutrition. *European Journal of Clinical Nutrition* 65, 743–749 **(2011)**

5. Dierdre A Kelly. Liver Complications of Pediatric Parenteral Nutrition—Epidemiology. *Nutrition* 14: 153-157 **(1998)**

6. Bernard Messing, Pascal Crenn, Philippe Beau, Marie Christine Boutron–Ruault, Jean–Claude Rambaud & Claude Matuchansky. Long-term survival and parenteral nutrition dependence in adult patients with the short bowel syndrome. *Gastroenterology* 117: 1043-1050 **(1999)**

7. James W. Keller, William R. C. Stewart, Robert Westerheide, William G. Pace. Prolonged survival with paired reversed segment after massive intestinal resection. *Archives of Surgery* 91(1): 174-179 **(1965)**

8. Budding J, Smith CC. Role of recirculating loops loops in the management of massive resection of the small intestine. *Surgery, Gynecology, Obstetrics* 125: 243-249 **(1967)**

9. Bobbie King, Gordon Carlson, Basem A. Khalil, Antonino MorabitoIntestinal. Bowel Lengthening in Children with Short Bowel Syndrome: Systematic Review of the Bianchi and STEP Procedures. *World Journal of Surgery* 37: 694-704 **(2013)**

10. Debra Sudan, Jon Thompson, Jean Botha, Wendy Grant, Dean Antonson, Steve Raynor, Alan Langnas. Comparison of intestinal lengthening procedures for patients with short bowel syndrome. *Annals of Surgery* 246: 593-604 **(200**7)

11. Alan L. Buchman, James Scolapio, Jon Fryer. AGA Technical Review on Short Bowel Syndrome and Intestinal Transplantation. *Gastroenterology* 124: 1111-1134 **(2003)**

12. R.S. Choi, J.P. Vacanti. Preliminary Studies of Tissue-Engineered Intestine Using Isolated Epithelial Organoid Units on Tubular Synthetic Biodegradable Scaffolds. *Transplantation Proceedings* 29: 848-851 **(1997)**

13. L. G. van der Flier, H. Clevers. Stem cells, self-renewal, and differentiation in the intestinal epithelium. *Annual Review of Physiology* 71: 241-260 **(2009)**

14. Nick Barker, Marc van de Wetering, and Hans Clevers. The intestinal stem cell. *Genes & Development* 22: 1856-1864 **(2008)**

15. Javier Mun˜ oz, Daniel E Stange, Arnout G Schepers, Marc van de Wetering, Bon-Kyoung Koo, Shalev Itzkovitz, Richard Volckmann, Kevin S Kung, Jan Koster, Sorina Radulescu, Kevin Myant, Rogier Versteeg, Owen J Sansom, Johan H van Es, Nick Barker, Alexander van Oudenaarden, Shabaz Mohammed, Albert JR Heck, and Hans Clevers. The Lgr5 intestinal stem cell signature: robust expression of proposed quiescent '+4' cell markers. *The EMBO Journal* 31: 3079–3091 **(2012)**

16. Andrea Haegebarth & Hans Clevers. Wnt Signaling, Lgr5, and Stem Cells in the Intestine and Skin. *The American Journal of Pathology* 174: 715-721 **(2009)**

17. Nick Barker, Johan H. van Es, Jeroen Kuipers, Pekka Kujala, Maaike van den Born, Miranda Cozijnsen, Andrea Haegebarth, Jeroen Korving, Harry Begthel, Peter J. Peters & Hans Clevers. Identification of stem cells in small intestine and colon by marker gene Lgr5. *Nature* 449:1003–1007 **(2007)**

18. Sangiorgi E, Capecchi MR. Bmi1 is expressed in vivo in intestinal stem cells. *Nature Genetics* 40:915–920 **(2008)**

19. Norifumi Takeda, Rajan Jain, Matthew R. LeBoeuf, Qiaohong Wang,
Min Min Lu, Jonathan A. Epstein. Interconversion between intestinal stem cell populations in distinct niches. *Science* 334:1420-1424 **(2011)**.

20. Robert K. Montgomery, Diana L. Carlone, Camilla A. Richmond, Loredana Farilla, Mariette E. G. Kranendonk, Daniel E. Henderson, Nana Yaa Baffour-Awuah, Dana M. Ambruzs, Laura K. Fogli, Selma Algra, David T. Breault and Robert A. Weinberg. Mouse telomerase reverse transcriptase (mTert) expression marks slowly cycling intestinal stem cells. *PNAS* 108:179-184 **(2011)**.

21. Anne E. Powell, Yang Wang, Yina Li, Emily J. Poulin, Anna L. Means, Mary K. Washington, James N. Higginbotham, Alwin Juchheim, Nripesh Prasad, Shawn E. Levy,Yan Guo, Yu Shyr, Bruce J. Aronow, Kevin M. Haigis, Jeffrey L. Franklin, and Robert J. Coffey. The pan-ErbB negative regulator Lrig1 is an intestinal stem cell marker that functions as a tumor suppressor. *Cell* 149:146–158 **(2012)**

22. Daniel Pinto, Hans Clevers. Wnt, stem cells and cancer in the intestine. *Biology of the Cell* 97: 185-196 **(2012)**

23. OLFM4 Is a Robust Marker for Stem Cells in Human Intestine and Marks a Subset of Colorectal Cancer Cells. *Gastroenterology* 137:15-17 **(2009)**

24. Li L, Clevers H. Coexistence of quiescent and active adult stem cells in mammals. *Science* 327:542–545 **(2010)**

25. Ryan G. Spurrier & Tracy C. Grikscheit. Tissue Engineering the Small Intestine. *Clinical Gasteroenterology and Hepatology* 11: 354-358 **(2013)**

26. Barker, N., van de Wetering, M. & Clevers, H. The intestinal stem cell. *Genes & Development* 22: 1856–1864 **(2008)**

27. Toshiro Sato, Robert G. Vries, Hugo J. Snippert, Marc van de Wetering, Nick Barker, Daniel E. Stange, Johan H. van Es, Arie Abo, Pekka Kujala, Peter J. Peters & Hans Clevers. Single Lgr5 stem cells build crypt–villus structures in vitro without a mesenchymal niche. *Nature* 459: 262-265 **(2009)**

28. Shiro Yui, Tetsuya Nakamura, Toshiro Sato, Yasuhiro Nemoto, Tomohiro Mizutani, Xiu Zheng, Shizuko Ichinose, Takashi Nagaishi, Ryuichi Okamoto, Kiichiro Tsuchiya, Hans Clevers & Mamoru Watanab. Functional engraftment of colon epithelium expanded in vitro from a single adult Lgr5+ stem cell. *Nature Medicine* 18: 618-624 **(2012)**

29. Robert P. Fordham, Shiro Yui, Nicholas R.F. Hannan, Christoffer Soendergaard, Alison Madgwick, Pawel J. Schweiger, Ole H. Nielsen, Ludovic Vallier, Roger A. Pedersen,Tetsuya Nakamura, Mamoru Watanabe, & Kim B. Jensen. Transplantation of Expanded Fetal Intestinal Progenitors Contributes to Colon Regeneration after Injury. *Cell Stem Cell* 13: 734-744 **(2013)**

30. Vatche G. Agopian, David C. Chen, Jeffrey R. Avansino, Matthias Stelzner. Intestinal Stem Cell Organoid Transplantation Generates Neomucosa in Dogs. *Journal of Gastrointestinal Surgery* 13: 971-982 **(2009)**

31. Anton Kuratnik & Charles Giardina. Intestinal organoids as tissue surrogates for toxicological and pharmacological studies. *Biochemical Pharmacology* 85: 1721-1726 **(2013)**

32. Daniel Pinto, Alex Gregorieff, Harry Begthel Hans Clevers. Canonical Wnt signals are essential for homeostasis of the intestinal epithelium. *Genes & Development* 17: 1709-1713 **(2003)**

33. Gijs R. van den Brink. Hedgehog signaling in development and homeostasis of the gastrointestinal tract. *American Physiological Society* 87: 1343-1375 **(2007)**

34. Kelli L. VanDussen, Alexis J. Carulli, Theresa M. Keeley, Sanjeevkumar R. Patel, Brent J. Puthoff, Scott T. Magness, Ivy T. Tran, Ivan Maillard, Christian Siebel, Åsa Kolterud, Ann S. Grosse, Deborah L. Gumucio, Stephen A. Ernst, Yu-Hwai Tsai, Peter J. Dempsey & Linda C. Samuelson . Notch signaling modulates proliferation and differentiation of intestinal crypt base columnar stem cells. *Development and Stem Cells* 139: 488-497 **(2012)**

35. Noboru Sato, Laurent Meijer, Leandros Skaltsounis, Paul Greengard & Ali H Brivanlou. Maintenance of pluripotency in human and mouse embryonic stem cells through activation of Wnt signaling by a pharmacological GSK-3-specific inhibitor. *Nature Medicine* 10:55-63 **(2004)**

36. Fengchao Wang, David Scoville, Xi C. He, Maxime M. Mahe, Andrew Box, John M. Perry, Nicholas R. Smith, Nan Ye Lei, Paige S. Davies, Megan K. Fuller, Jeffrey S. Haug, Melainia Mcclain, Adam D. Gracz, Sheng Ding, Matthias Stelzner, James C. Y. Dunn, Scott T. Magness, Melissa H. Wong, Martin G. Martin, Michael Helmrath Linheng Li. Isolation and Characterization of Intestinal Stem Cells Based on Surface Marker Combinations and Colony-Formation Assay. *Gastroenterology* 145: 383-395 **(2013)**

37. Xianjun Fang, Shuang Xing Yu, Yiling Lu, Robert C. Bast, Jr., James R. Woodgett, and Gordon B. Mills. Phosphorylation and inactivation of glycogen synthase kinase 3 by protein kinase A. *PNAS* 97: 11960-11965 **(2000)**

38. Xi He. A wnt-wnt situation. Developmental Cell 4: 791-797 **(2003)**

39. Edward A. Dennis, Ralph A. Bradshaw. Intercellular Signaling in Development and Disease: Cell Signaling Collection **(2011)**

40. Ana Martinez, Ana Castro, Isabel Dorronsoro, Mercedes Alonso. Glycogen synthase kinase 3 (GSK-3) inhibitors as new promising drugs for diabetes, neurodegeneration, cancer, and inflammation. *Medicinal Research Reviews* 22: 373-384 **(2002)**

41. Abbas Shakoori, Andrei Ougolkov, Zhi Wei Yu, Bin Zhang, Mohammad H. Modarressi, Daniel D. Billadeau, Masayoshi Mai, Yutaka Takahashi, Toshinari Minamoto. Deregulated GSK3b activity in colorectal cancer: Its association with tumor cell survival and proliferation. *Biochemical and Biophysical Research Communications* 334:1365–1373 **(2005)**

42. Fabienne Danhier, Eduardo Ansorena, Joana M. Silva, Régis Coco, Aude Le Breton, Véronique Préat. PLGA-based nanoparticles: An overview of biomedical applications. *Journal of Controlled Release* 161: 505-522 **(2012)**

43. Siti M. Janib, Ara S. Moses, J. Andrew MacKay. Imaging and drug delivery using theranostic nanoparticles. *Advanced Drug Delivery Reviews* 62: 1052-1063 **(2010)**

44. N. Schleicha, P. Sibretb, P. Danhierc, B. Ucakara, S. Laurentd, R.N. Mullerd,e, C. Jérômeb,

B. Gallezc, V. Préat, F. Danhiera. Dual anticancer drug/superparamagnetic iron oxide-loaded PLGA-based nanoparticles for cancer therapy and magnetic resonance imaging.International *Journal of Pharmaceutics* 447: 94-101 **(2013)**

45. Loran D. Solorio, Andrew S. Fu,Roberto Herna´ndez-Irizarry, Eben Alsberg. Chondrogenic differentiation of human mesenchymal stem cell aggregates via controlled release of TGF-b1 from incorporated polymer microspheres. *Journal of Biomedical Materials Research* 92: 1139-1144 **(2010)**

46. Bon-Kyoung Koo, Daniel E Stange, Toshiro Sato, Wouter Karthaus1, Henner F Farin, Meritxell Huch, Johan H van Es & Hans Clevers Controlled gene expression in primary Lgr5 organoid cultures. *Nature Methods* 9: 81-83 **(2012)**

47. Kiichi Watanabe, Morio Ueno, Daisuke Kamiya, Ayaka Nishiyama, Michiru Matsumura, Takafumi Wataya, Jun B Takahashi, Satomi Nishikawa, Shin-ichi Nishikawa, Keiko Muguruma & Yoshiki Sasai. A ROCK inhibitor permits survival of dissociated human embryonic stem cells. *Nature Biotechnology* 25: 681-686 **(2007)**

48. Xiangyun Li, Roman Krawetz, Shiying Liu, Guoliang Meng, & Derrick E. Rancourt. ROCK inhibitor improves survival of cryopreserved serum/feeder-free single human embryonic stem cells. *Human Reproduction* 24: 580-289 **(2004)**

49. Henner F. Farin, Johan H. Van Es, & Hans Clevers. Redundant Sources of Wnt Regulate Intestinal Stem Cells and Promote Formation of Paneth Cells. *Gastroenterology* 143: 1518-1529 **(2012)**

50. Toshiro Sato, Johan H. van Es, Hugo J. Snippert, Daniel E. Stange, Robert G. Vries, Maaike van den Born, Nick Barker, Noah F. Shroyer, Marc van de Wetering & Hans Clevers. Paneth cells constitute the niche for Lgr5 stem cells in intestinal crypts. *Nature* 469: 415-418 **(2011)**

51. Yongyan Wu, Zhiying Ai, Kezhen Yao, Lixia Cao, Juan Du, Xiaoyan Shi, Zekun Guo &Yong Zhang. CHIR99021 promotes self-renewal of mouse embryonic stem cells by modulation of protein-encoding gene and long intergenic non-coding RNA expression. *Experimental Cell Research* 319: 2684-2689 **(2013)**

52. Nick barker. Adult intestinal stem cells: critical drivers of epithelial homeostasis and regeneration. *Nature Review Molecular Cell Biology* 15: 19-33 **(2014)**

53. Xiaolei Yin, Henner F Farin, Johan H van Es, Hans Clevers, Robert Langer & Jeffrey M Karp. Niche-independent high-purity cultures of Lgr5+ intestinal stem cells and their progeny. *Nature Methods* 11: 106-112 **(2014)**